CAVS REPORT
MSU.CAVS.CMD.2007-R0015
Confidential
Printed September 2007

On Developing a Viscoelastic-Viscoplastic Model for Polymeric Materials

E. B. Marin, R. Prabhu, M. F. Horstemeyer

Prepared by
Center for Advanced Vehicular Systems
Mississippi State University
Mississippi State, MS 39762

Web site: http://www.cavs.msstate.edu

September 2007

Distribution List:

Paul Decker (TARDEC)
Thomas Udvare (TARDEC)
David Gorsich (TARDEC)
Jim Dusett (TARDEC)
David Lamb (TARDEC)
Mike Letherwood (TARDEC)
Benton Gady (TARDEC)
Theodore Currier (TARDEC)
Mark Horstemeyer (MSU)
mfhorst@me.msstate.edu
Paul Wang (MSU)
pwang@cavs.msstate.edu
Rand German (MSU)
german@cavs.msstate.edu
Jean Luc Bouvard (MSU)
jeanluc@cavs.msstate.edu
Gabriel Potirniche (MSU)
gabriel@cavs.msstate.edu
Yibin (Anna) Xue (MSU)
axue@cavs.msstate.edu
Tom Lacy (MSU)
lacy@ae.msstate.edu
Jilei Zhang (MSU)
jzhang@cfr.msstate.edu
Sheldon Shi (MSU)
sshi@cfr.msstate.edu

TARDEC Address:
6501 E. 11 Mile Rd.
Warren, MI 483997-5000

On Developing a Viscoelastic–Viscoplastic Model for Polymeric Materials

Esteban B. Marin, Raj Prabhu, Mark F. Horstemeyer
Center For Advanced Vehicular Systems
Mississippi State University
P.O. Box 5405
Mississippi State, MS 39762

Abstract

This report presents the formulation of a three-dimensional, finite deformation, isothermal, viscoelastic-viscoplastic constitutive model for (thermoplastic) amorphous polymeric materials. The formulation follows a widely used theory for amorphous polymers as described by [Boyce *et al.*, 1988], with the development framed in a thermodynamic setting as presented by [Anand and Ames, 2006]. Conceptually, the main features of the model can be described with a typical rheological model: a nonlinear Maxwell element in parallel with a nonlinear (hyperelastic) spring. The constitutive equations of the model are specialized to the one–dimensional case. The numerical integration of the one–dimensional equations and corresponding implementation in MATLAB are described. This implementation is then used to perform a parametric study of the model. This study shows that this initial version of the model reproduces typical features experimentally observed in the stress response of many amorphous polymeric materials.

Keywords: viscoelasticity, viscoplasticity, finite deformation, constitutive integration, polymeric materials.

Contents

List of Figures

1. Introduction

Polymeric materials have been extensively used in a broad range of applications; including aerospace and automotive industries. Due to the increased use of polymers, much research has focused on developing continuum material models to understand their brittle, viscoelastic, viscoplastic and rubbery response under different loading conditions. At CAVS research efforts in this direction have been recently initiated, work that have been triggered by a number of research activities concerning the material behavior of polymeric–type materials. In this respect, this report documents the initial modeling efforts in this area.

In general, polymers exhibit a rich variety of material behavior which is very temperature and rate dependent. Such behavior is mainly due to their particular microstucture. Extensively intertwined, long molecular chains have backbone bonds which permit rotation, but very little extension. At temperatures well below the glass transition, backbone bonds are rigid and the network is stiffly interlocked, resulting in a brittle response. At higher temperatures, in a narrow range centered about the glass transition, backbone bonds are able to rotate to varying degrees, allowing molecules to partially disentangle and move (slip) relative to one another. This results in a variety of viscoelastic-viscoplastic behaviors. At temperatures well above the glass transition backbone bonds rotate easily allowing complete disentanglement. Cross linked polymers retain some rigidity because of the bonding between molecules, resulting in a rubbery behavior. On the other hand, uncross-linked polymers flow viscously. To capture such a wide range of responses, a number of constitutive models have been developed in the open literature. In particular, many physically-based constitutive equations based on differential formulations using internal state variables have been proposed [Boyce *et al.*, 1988; Anand, 1996; Bardenhagen *et al.*, 1997; Reese and Govindjee, 1998; Anand and Gurtin, 2003; Kontou, 2006; Anand and Ames, 2006].

In this report, we present the formulation of a constitutive framework focused on modeling the response of polymers under isothermal deformations at temperatures below and close to the glass transition temperature (thermoplastics with amorphous structure). As mentioned above, in this regime the mechanical response of polymers present features of viscoelastic and viscoplastic behaviors that has been widely documented in the literature [Zairi, *et al.*, 2007]. The presented formulation is based on a differential formulation using internal state variables and follows closely a widely used theory for amorphous polymers [Boyce *et al.*, 1988], with the development framed in a thermodynamic setting [Anand and Ames, 2006]. Conceptually, the main features of the model can be described with a typical one-dimensional rheological model: a nonlinear Maxwell element in parallel with a nonlinear (hyperelastic)

spring.

The presentation proceeds by describing the constitutive modeling of a simple one-dimensional linear viscoelastic solid that will set the stage for the methodology used for formulating the constitutive framework. Next, the large deformation kinematics and thermodynamics used to formulate the three-dimensional material model is presented. This is followed by the development of the constitutive equations of the model. These equations are then simplified to the one-dimensional case whose numerical integration is described in detail. The numerical implementation of this integration scheme in MATLAB is then used to carry out a parametric study of the model.

The work uses Gibb's (direct) notation [Gurtin, 1981] to express tensor quantities and their mathematical operations. Consider for example the two second order tensors $\boldsymbol{A}$ and $\boldsymbol{B}$. Tensor operations between the tensors $\boldsymbol{A}$ and $\boldsymbol{B}$ are indicated as $\boldsymbol{AB}$ for the inner product (a second order tensor), $\boldsymbol{A} \otimes \boldsymbol{B}$ for the dyadic product (a fourth order tensor), and $\boldsymbol{A}{:}\boldsymbol{B}$ for the scalar product (a scalar). Any other particular tensor notation used in the development will be either clear from the context or noted in the text.

2. A Simple Viscoelastic Model

In order to set the stage for the development of the model, in this section we present the formulation of a simple one-dimensional rheological (spring-dashpot) model, the standard linear solid. The standard linear solid consists of a linear spring and dashpot in series (a Maxwell element) in parallel with a linear spring, see Fig. 2.1. The formulation of the constitutive equations of the model is carried out assuming small deformations and using a thermodynamics formalism. The extension of this methodology to the three dimensional finite deformation case is presented in the next section, extension that will also account for nonlinear (inelasticty) effects on the material response, as presented by a number of authors [Boyce, *et al.*, 1988; Reese and Govindjee, 1998; Kontou, 2006; Anand and Ames, 2006].

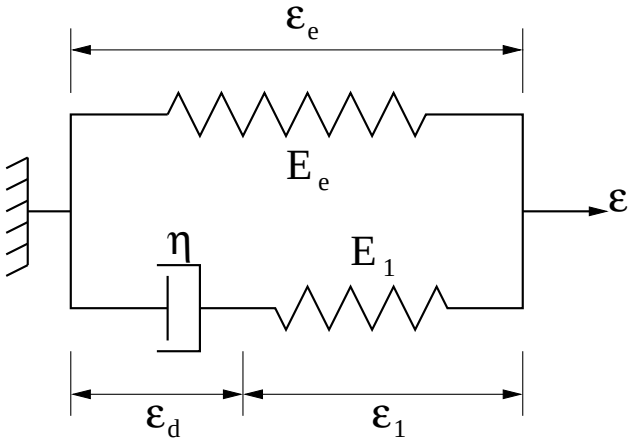

Figure 2.1: A simple viscoelastic model: the standard linear solid.

The kinematics for this simple model can be written as

$$\epsilon = \epsilon_e = \epsilon_1 + \epsilon_d \tag{2.1}$$

where ϵ is the applied strain, (ϵ_e, ϵ_1) are the elastic strains in the springs, and ϵ_d is the inelastic strain in the dashpot. On the other hand, the mechanical version of the dissipitation inequality can be expressed as [Coleman and Gurtin, 1967]

$$-\dot{\psi} + \sigma\dot{\epsilon} \geq 0 \tag{2.2}$$

where σ is the total stress in the system, and ψ is the Helmholtz free energy associated with the arrangement in Fig. 2.1. Here we assume that free energy depends on the elastic strains (ϵ_e, ϵ_1), and hence its time derivative can be computed as

$$\psi = \hat{\psi}(\epsilon_e, \epsilon_1) \qquad \rightarrow \qquad \dot{\psi} = \frac{\partial \hat{\psi}}{\partial \epsilon_e}\dot{\epsilon}_e + \frac{\partial \hat{\psi}}{\partial \epsilon_1}\dot{\epsilon}_1 \tag{2.3}$$

where the rates of strain can be related by

$$\dot{\epsilon} = \dot{\epsilon}_e, \qquad \dot{\epsilon}_1 = \dot{\epsilon}_e - \dot{\epsilon}_d \tag{2.4}$$

Substituting Eqs.(2.3) and (2.4) into Eq.(2.2) and grouping terms, one obtains

$$\Big(- \underbrace{\frac{\partial \hat{\psi}}{\partial \epsilon_e}}_{\sigma_e} - \underbrace{\frac{\partial \hat{\psi}}{\partial \epsilon_1}}_{\sigma_1} + \sigma \Big)\dot{\epsilon}_e + \underbrace{\frac{\partial \hat{\psi}}{\partial \epsilon_1}}_{\sigma_1 = \sigma_d} \dot{\epsilon}_d \geq 0 \tag{2.5}$$

where σ_e and σ_1 are the stresses in the springs, and σ_d is the (dissipative) stress in the dashpot. Note here that, in the literature, σ_e and σ_1 are also called the equilibrium σ_{EQ} and non-equilibrium σ_{NEQ} stresses [Reese and Govindjee, 1998]. Using standard arguments one obtains from Eq.(2.5)

$$\sigma = \sigma_e + \sigma_1 \tag{2.6}$$

$$\sigma_d \, \dot{\epsilon}_d \geq 0 \tag{2.7}$$

where Eq.(2.6), derived from thermodynamic arguments, gives the balance between the applied stress and the stresses in the springs, and Eq.(2.7) establishes that dissipation is nonnegative.

Specific constitutive equations for the springs can be obtained assuming the following form for the free energy (Hookean springs)

$$\hat{\psi}(\epsilon_e, \epsilon_1) = \frac{1}{2}E_e\epsilon_e^2 + \frac{1}{2}E_1\epsilon_1^2 \tag{2.8}$$

from which the constitutive equations for the springs can be computed as

$$\sigma_e \; = \; \frac{\partial \hat{\psi}}{\partial \epsilon_e} = E_e\epsilon_e \tag{2.9}$$

$$\sigma_1 \; = \; \frac{\partial \hat{\psi}}{\partial \epsilon_1} = E_1\epsilon_1 = E_1(\epsilon_e - \epsilon_d) \tag{2.10}$$

Also, assuming a linear–Newtonian– dashpot with a (constant) viscocity coefficient η, the dissipation inequality results

$$\sigma_d = \eta\dot{\epsilon}_d \qquad \rightarrow \qquad \sigma_d\dot{\epsilon}_d = \eta(\dot{\epsilon}_d)^2 \geq 0 \tag{2.11}$$

which implies that $\eta \geq 0$.

Then, the constitutive equations for the simple viscoelastic model depicted in Fig. 2.1 can be summarized by

$$\begin{aligned} \epsilon &= \epsilon_e = \epsilon_1 + \epsilon_d \\ \sigma &= \sigma_e + \sigma_1 \\ \sigma_e &= E_e \epsilon_e, \qquad \sigma_1 = E_1(\epsilon_e - \epsilon_d) \\ \sigma_1 &= \sigma_d = \eta \dot{\epsilon}_d \end{aligned} \tag{2.12}$$

Note that by eliminating the strains ϵ_e and ϵ_1 from these equations, one can obtain the differential form of the model as

$$\sigma = E_0 \epsilon - E_1 \epsilon_d \tag{2.13}$$

$$\dot{\epsilon_d} + \frac{1}{\tau}\epsilon_d = \frac{1}{\tau}\epsilon \tag{2.14}$$

where $E_0 = E_e + E_1$ and $\tau = \eta / E_1$. The (hereditary) integral representation of the model can be derived by integrating Eq.(2.14) to obtain $\epsilon_d(t)$ and subtituting the resulting equation into Eq.(2.13), to give

$$\sigma(t) = \int_{-\infty}^{t} G(t-s)\dot{\epsilon}(s)ds, \qquad G(t) = E_e + E_1 \exp\left(\frac{-t}{\tau}\right) \tag{2.15}$$

where $G(t)$ is called the relaxation modulus. Note that, based on the above methodology, the transformation from the differential to the integral form was facilitated by the linearity of the model (linear springs and linear dashpot). When nonlinearities are introduced in the model (e.g. inelasticity), such transformation may not be possible. In such a case, one should favor the differential representation of the model.

3. Constitutive Model for Amorphous Polymers

In this section we derive a large deformation three-dimensional constitutive model for the isothermal nonlinear viscoelastic-viscoplastic response of amorphous polymeric materials. The model follows a widely used theory for amorphous polymers as described by [Boyce *et al.*, 1988], with the development framed in a thermodynamic setting as presented by [Anand and Ames, 2006]. Conceptually, the main features of the model can be described by the rheological model presented in Fig. 3.1. As indicated by this figure, the model consists of a nonlinear Maxwell element (branch A, non-equilibrium component) connected in parallel with a Langevin spring (branch B, equlibrium component). The Maxwell component involves a nonlinear elastic spring to represent elastic molecular interactions, and a nonlinear viscous dashpot to account for the non-newtonian viscoplastic flow arising from the motion of polymer segments (unkinking and sliding). On the other hand, the rubber-elastic Langevin spring, a concept derived from a non-Gaussian statistical mechanics theory of rubber elasticity [Arruda and Boyce, 1993], models the post-yield strain hardening at large strains due to the alignment of the long-chain polymer molecules.

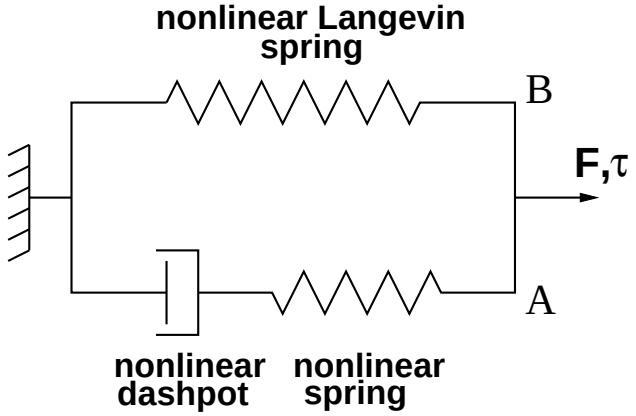

Figure 3.1: Schematic representation of nonlinear rheological model for amorphous polymers.

In what follows, we describe the large deformation kinematics and the thermodynamic setting of the model, aspects that are used to develop the three-dimensional constitutive equations. In a latter section, we present the one-dimensional version (uniaxial extension)

of the equations and the corresponding integration scheme. The corresponding numerical implementation in MATLAB is then used to perform a parametric study of the model.

3.1 Kinematics

The arrangement of the model elements presented in Fig. 3.1 indicates that the total deformation gradient $\boldsymbol{F}$ is applied to both branches (deformation–driven problem), i.e.,

$$\boldsymbol{F} = \boldsymbol{F}_A = \boldsymbol{F}_B \tag{3.1}$$

Branch B, which describes the rubbery behavior of the material by means of a Langevin spring, is modeled using hyperelasticity, and hence, its deformation is fully defined by $\boldsymbol{F}$. However, the response of branch A, which should capture inelasticity effects on the material response, is represented using the multiplicative decomposition of $\boldsymbol{F}$ into elastic and plastic (inelastic) components

$$\boldsymbol{F} = \boldsymbol{F}^e\boldsymbol{F}^p, \quad J = \det\boldsymbol{F} = J^eJ^p = J^e > 0, \quad J^e = \det\boldsymbol{F}^e, \quad J^p = \det\boldsymbol{F}^p = 1 \tag{3.2}$$

As described by [Anand and Ames, 2006], $\boldsymbol{F}^p$ represents a local plastic (isochoric) deformation of the material due to plastic mechanisms such as stretching, rotation and relative slippage of the molecular chains, while $\boldsymbol{F}^e$ represents elastic mechanisms such as strectching and rotation of the intermolecular structure. Note that decomposition (3.2) suggests that there exist an intermediate configuration between the undeformed $\mathcal{B}_0$ and the current $\mathcal{B}$ configurations, which is denoted here by $\bar{\mathcal{B}}$. Hypothetically, $\bar{\mathcal{B}}$ is obtained from $\mathcal{B}$ by unloading through $\boldsymbol{F}^{e-1}$ to a zero stress state (a relaxed configuration). Using Eq.(3.2), we can compute the velocity gradient $\boldsymbol{l}$ in $\mathcal{B}$ as

$$\boldsymbol{l} = \dot{\boldsymbol{F}}\boldsymbol{F}^{-1} = \boldsymbol{l}^e + \boldsymbol{F}^e\bar{\boldsymbol{L}}^p\boldsymbol{F}^{e-1}, \qquad \bar{\boldsymbol{L}}^p = \dot{\boldsymbol{F}}^p\boldsymbol{F}^{p-1} \tag{3.3}$$

where $\boldsymbol{l}^e = \dot{\boldsymbol{F}}^e\boldsymbol{F}^{e-1}$. Note that $\boldsymbol{l}^e$ and $\bar{\boldsymbol{L}}^p$ can be decomposed into their symmetric and skew parts, i.e., $\boldsymbol{l}^e = \boldsymbol{d}^e + \boldsymbol{w}^e$ and $\bar{\boldsymbol{L}}^p = \bar{\boldsymbol{D}}^p + \bar{\boldsymbol{W}}^p$. Here we take $\bar{\boldsymbol{W}}^p = \boldsymbol{0}$, a reasonable assumption for solids that are isotropic-viscoplastic or amorphous [Gurtin and Anand, 2005]. Hence, $\bar{\boldsymbol{L}}^p = \bar{\boldsymbol{D}}^p$.

As an aside, we note that the Cauchy stresses in branches A and B, denoted here as $\boldsymbol{\sigma}_A$ and $\boldsymbol{\sigma}_B$, respectively, can be written as [Holzapfel, 2000]

$$\boldsymbol{\sigma}_A = J^{e-1}\boldsymbol{\tau}_A = J^{e-1}\boldsymbol{F}^e\bar{\boldsymbol{S}}_A\boldsymbol{F}^{eT}, \qquad \boldsymbol{\sigma}_B = J^{-1}\boldsymbol{\tau}_B = J^{-1}\boldsymbol{F}\boldsymbol{S}_B\boldsymbol{F}^T, \tag{3.4}$$

where $\boldsymbol{\tau}_A$ and $\boldsymbol{\tau}_B$ are the Kirchhoff stresses in branches A and B and $\bar{\boldsymbol{S}}_A$ and $\boldsymbol{S}_B$ are the corresponding second Piola-Kirchhoff stresses expressed in configurations $\bar{\mathcal{B}}$ and $\mathcal{B}_0$, respectively. Note that $\boldsymbol{\tau}_A$ is defined by a force per unit volume in $\bar{\mathcal{B}}$ and $\boldsymbol{\tau}_B$ is a force per unit volume of $\mathcal{B}_0$. However, since $J = J^e$, Eq.(3.2), both volumes should be the same. Also, as shown below, the Kirchhoff stresses in each branch are related to the overall Kirchhoff stress $\boldsymbol{\tau}$ by $\boldsymbol{\tau} = \boldsymbol{\tau}_A + \boldsymbol{\tau}_B$, which translates to $\boldsymbol{\sigma} = \boldsymbol{\sigma}_A + \boldsymbol{\sigma}_B$.

3.2 Thermodynamics

The mechanical version of the global dissipitation (Clausius-Duhem) inequality asserts that temporal changes in the total free energy be no greater than the rate at which total work is performed. Mathematically this statement can be written as [Gurtin and Anand, 2005] *

$$-\frac{D}{Dt}\int_{\mathcal{B}}\Psi dv = -\int_{\mathcal{B}} J^{-1}\dot{\bar{\Psi}}dv \geq \int_{\mathcal{B}}\boldsymbol{\sigma}\!:\!\boldsymbol{l}dv \tag{3.5}$$

where Ψ and $\bar{\Psi}$ denote the Helmholtz free energy per unit volume in the current $\mathcal{B}$ and relaxed $\bar{\mathcal{B}}$ configurations, respectively. Note here that, if we denote Ψ_0 the free energy per unit volume in $\mathcal{B}_0$, one can write $\bar{\Psi} = \Psi_0$ since $J^p = 1$. In Eq.(3.5), the stress power per unit volume in $\mathcal{B}$ can be expressed as

$$\begin{aligned}\boldsymbol{\sigma}\!:\!\boldsymbol{l} &= \boldsymbol{\sigma}\!:\!\boldsymbol{l}^e + J^{-1}\boldsymbol{F}^e\bar{\boldsymbol{S}}\boldsymbol{F}^{eT}\!:\!\boldsymbol{F}^e\bar{\boldsymbol{L}}^p\boldsymbol{F}^{e-1}\\ &= \boldsymbol{\sigma}\!:\!\boldsymbol{l}^e + J^{-1}\bar{\boldsymbol{C}}^e\bar{\boldsymbol{S}}\!:\!\bar{\boldsymbol{L}}^p\\ &= \boldsymbol{\sigma}\!:\!\boldsymbol{d}^e + J^{-1}\bar{\boldsymbol{M}}\!:\!\bar{\boldsymbol{D}}^p\end{aligned} \tag{3.6}$$

where $\bar{\boldsymbol{M}} = \bar{\boldsymbol{C}}^e\bar{\boldsymbol{S}}$ is the Mandel stress, with $\bar{\boldsymbol{C}}^e = \boldsymbol{F}^{eT}\boldsymbol{F}^e$ being the elastic Cauchy-Green tensor. In this last equation we have used Eq.(3.3), the decomposition $\boldsymbol{l}^e = \boldsymbol{d}^e + \boldsymbol{w}^e$, the symmetry of $\boldsymbol{\sigma}$, the relationship $\boldsymbol{\sigma} = J^{e-1}\boldsymbol{\tau} = J^{-1}\boldsymbol{F}^e\bar{\boldsymbol{S}}\boldsymbol{F}^{eT}$, and the fact that $\bar{\boldsymbol{L}}^p = \bar{\boldsymbol{D}}^p$ ($\bar{\boldsymbol{W}}^p = 0$). Substituting Eq.(3.6) into Eq.(3.5), one obtains

$$\int_{\mathcal{B}} J^{-1}(-\dot{\bar{\Psi}} + \boldsymbol{\tau}\!:\!\boldsymbol{d}^e + \bar{\boldsymbol{M}}\!:\!\bar{\boldsymbol{D}}^p)dv \geq 0 \tag{3.7}$$

The local form of the dissipitation inequality can be obtained by localizing the above integral equation, resulting in

$$\boldsymbol{\tau}\!:\!\boldsymbol{d}^e + \bar{\boldsymbol{M}}\!:\!\bar{\boldsymbol{D}}^p - \dot{\bar{\Psi}} \geq 0 \tag{3.8}$$

*Elemental volumes in configurations $\mathcal{B}_0$ (dV), $\bar{\mathcal{B}}$ ($d\bar{V}$), and $\mathcal{B}$ (dv) are related by $dv = J^e d\bar{V} = JdV$. In addition, $d\bar{V} = J^p dV = dV$ since $J^p = 1$. Hence, denoting $\bar{\Psi}$ the free energy per unit volume in $\bar{\mathcal{B}}$.

$$\int_{\bar{\mathcal{B}}}\bar{\Psi}d\bar{V} = \int_{\mathcal{B}}\bar{\Psi}J^{e-1}dv = \int_{\mathcal{B}}\bar{\Psi}J^{-1}dv = \int_{\mathcal{B}}\Psi dv$$

Therefore,

$$\frac{D}{Dt}\int_{\mathcal{B}}\Psi dv = \frac{D}{Dt}\int_{\bar{\mathcal{B}}}\bar{\Psi}d\bar{V} = \frac{D}{Dt}\int_{\mathcal{B}_0}\bar{\Psi}J^p dV = \int_{\bar{\mathcal{B}}}(\dot{\bar{\Psi}} + \bar{\Psi}\mathrm{tr}(\bar{\boldsymbol{L}}^p))d\bar{V} = \int_{\bar{\mathcal{B}}}\dot{\bar{\Psi}}d\bar{V}$$

where $\mathrm{tr}(\boldsymbol{L}^p) = \dot{J}^p/J^p = 0$. Finally, since $d\bar{V} = J^{e-1}dv = J^{-1}dv$, then

$$\frac{D}{Dt}\int_{\mathcal{B}}\Psi dv = \int_{\mathcal{B}}\dot{\bar{\Psi}}J^{-1}dv$$

Following existing theories [Reese and Govindjee, 1998; Anand and Ames, 2006], we assume that the Helmholtz free energy, typically an isotropic function of its arguments, depends on the independent variables $\bar{\boldsymbol{C}}^e$ and the Cauchy-Green tensor $\boldsymbol{C} = \boldsymbol{F}^T\boldsymbol{F}$, i.e.,

$$\bar{\Psi} = \hat{\bar{\Psi}}(\bar{\boldsymbol{C}}^e, \boldsymbol{C}) \tag{3.9}$$

and, hence, its time derivative can be computed as

$$\dot{\bar{\Psi}} = \frac{\partial \hat{\bar{\Psi}}}{\partial \bar{\boldsymbol{C}}^e} : \dot{\bar{\boldsymbol{C}}}^e + \frac{\partial \hat{\bar{\Psi}}}{\partial \boldsymbol{C}} : \dot{\boldsymbol{C}} \tag{3.10}$$

The first term of this equation can be evaluated as

$$\frac{\partial \hat{\bar{\Psi}}}{\partial \bar{\boldsymbol{C}}^e} : \dot{\bar{\boldsymbol{C}}}^e = \frac{\partial \hat{\bar{\Psi}}}{\partial \bar{\boldsymbol{C}}^e} : (\dot{\boldsymbol{F}}^{eT}\boldsymbol{F}^e + \boldsymbol{F}^{eT}\dot{\boldsymbol{F}}^e) = 2\boldsymbol{F}^e \frac{\partial \hat{\bar{\Psi}}}{\partial \bar{\boldsymbol{C}}^e}\boldsymbol{F}^{eT} : \underbrace{\dot{\boldsymbol{F}}^e\boldsymbol{F}^{e-1}}_{\boldsymbol{l}^e} = 2\boldsymbol{F}^e \frac{\partial \hat{\bar{\Psi}}}{\partial \bar{\boldsymbol{C}}^e}\boldsymbol{F}^{eT} : \boldsymbol{d}^e \tag{3.11}$$

while the second term can be reduced to

$$\begin{aligned}\frac{\partial \hat{\bar{\Psi}}}{\partial \boldsymbol{C}} : \dot{\boldsymbol{C}} = \frac{\partial \hat{\bar{\Psi}}}{\partial \boldsymbol{C}} : (\dot{\boldsymbol{F}}^T\boldsymbol{F} + \boldsymbol{F}^T\dot{\boldsymbol{F}}) = 2\boldsymbol{F}\frac{\partial \hat{\bar{\Psi}}}{\partial \boldsymbol{C}}\boldsymbol{F}^T : \underbrace{\dot{\boldsymbol{F}}\boldsymbol{F}^{-1}}_{\boldsymbol{l}} \\ = 2\boldsymbol{F}\frac{\partial \hat{\bar{\Psi}}}{\partial \boldsymbol{C}}\boldsymbol{F}^T : \boldsymbol{d}^e + \bar{\boldsymbol{C}}^e\boldsymbol{F}^{e-1}(2\boldsymbol{F}\frac{\partial \hat{\bar{\Psi}}}{\partial \boldsymbol{C}}\boldsymbol{F}^T)\boldsymbol{F}^{e-T} : \bar{\boldsymbol{D}}^p\end{aligned} \tag{3.12}$$

where we have used Eq.(3.3) together with $\boldsymbol{l}^e = \boldsymbol{d}^e + \boldsymbol{w}^e$ and the symmetry of $\partial\bar{\Psi}/\partial\bar{\boldsymbol{C}}^e$ and $\partial\bar{\Psi}/\partial\boldsymbol{C}$. Substituting Eqs.(3.10) together with Eqs.(3.11) and (3.12) into the dissipitation inequality, Eq.(3.8), we obtain

$$\Big[\boldsymbol{\tau} - \boldsymbol{F}^e \underbrace{2\frac{\partial \hat{\bar{\Psi}}}{\partial \bar{\boldsymbol{C}}^e}}_{\bar{\boldsymbol{S}}_A}\boldsymbol{F}^{eT} - \boldsymbol{F}\underbrace{2\frac{\partial \hat{\bar{\Psi}}}{\partial \boldsymbol{C}}}_{\boldsymbol{S}_B}\boldsymbol{F}^T\Big] : \boldsymbol{d}^e + \Big[\bar{\boldsymbol{M}} - \bar{\boldsymbol{C}}^e\boldsymbol{F}^{e-1}(\boldsymbol{F}\underbrace{2\frac{\partial \hat{\bar{\Psi}}}{\partial \boldsymbol{C}}}_{\boldsymbol{S}_B}\boldsymbol{F}^T)\boldsymbol{F}^{e-T}\Big] : \bar{\boldsymbol{D}}^p \geq 0 \tag{3.13}$$

Using standard arguments [Coleman and Gurtin, 1967], we obtain from the first term

$$\boldsymbol{\tau} = \boldsymbol{\tau}_A + \boldsymbol{\tau}_B, \qquad \boldsymbol{\tau}_A = \boldsymbol{F}^e\bar{\boldsymbol{S}}_A\boldsymbol{F}^{eT} \qquad \boldsymbol{\tau}_B = \boldsymbol{F}\boldsymbol{S}_B\boldsymbol{F}^T \tag{3.14}$$

What is left for the dissipitation inequality is then

$$\Big[\bar{\boldsymbol{M}} - \bar{\boldsymbol{C}}^e\boldsymbol{F}^{e-1}\boldsymbol{\tau}_B\boldsymbol{F}^{e-T}\Big] : \bar{\boldsymbol{D}}^p \geq 0 \tag{3.15}$$

Replacing the expression fot the Mandel stress, $\bar{\boldsymbol{M}} = \bar{\boldsymbol{C}}^e\bar{\boldsymbol{S}} = \bar{\boldsymbol{C}}^e\boldsymbol{F}^{e-1}\boldsymbol{\tau}\boldsymbol{F}^{e-T}$, in the above equation, one gets for the reduced dissipitation inequality

$$\bar{\boldsymbol{C}}^e \underbrace{\boldsymbol{F}^{e-1}\overbrace{(\boldsymbol{\tau} - \boldsymbol{\tau}_B)}^{\boldsymbol{\tau}_A}\boldsymbol{F}^{e-T}}_{\bar{\boldsymbol{S}}_A} : \bar{\boldsymbol{D}}^p \geq 0 \qquad \rightarrow \qquad \bar{\boldsymbol{M}}_A : \bar{\boldsymbol{D}}^p \geq 0 \tag{3.16}$$

where $\bar{\boldsymbol{M}}_A = \bar{\boldsymbol{C}}^e\bar{\boldsymbol{S}}_A$ is the Mandel stress in branch A. Note that Eqs.(3.14) and (3.16) are the three-dimensional counterparts of Eqs.(2.6) and (2.7), respectively.

3.3 Model Equations

Without loss of generality, we additively decomposed the free energy as

$$\hat{\bar{\Psi}}(\bar{\boldsymbol{C}}^e, \boldsymbol{C}) = \hat{\bar{\Psi}}_e(\bar{\boldsymbol{C}}^e) + \hat{\bar{\Psi}}_C(\boldsymbol{C}) \tag{3.17}$$

Then the 2nd Piola-Kirchhoff stresses in Eq.(3.14) can be computed using

$$\bar{\boldsymbol{S}}_A = 2\frac{\partial \hat{\bar{\Psi}}_e}{\partial \bar{\boldsymbol{C}}^e} \qquad \boldsymbol{S}_B = 2\frac{\partial \hat{\bar{\Psi}}_C}{\partial \bar{\boldsymbol{C}}} \tag{3.18}$$

To develop the expression for the stress in branch A, we start by using the polar decomposition of $\boldsymbol{F}^e$

$$\boldsymbol{F}^e = \boldsymbol{R}^e\boldsymbol{U}^e, \qquad \bar{\boldsymbol{C}}^e = \boldsymbol{F}^{eT}\boldsymbol{F}^e = \boldsymbol{U}^{e2} \tag{3.19}$$

and by writing the spectral representation of $\boldsymbol{U}^e$ and $\bar{\boldsymbol{C}}^e$ as

$$\boldsymbol{U}^e = \sum_{\bar{I}=1}^{3} \lambda^e_{\bar{I}} \bar{\boldsymbol{n}}_{\bar{I}} \otimes \bar{\boldsymbol{n}}_{\bar{I}}, \qquad \bar{\boldsymbol{C}}^e = \boldsymbol{U}^{e2} = \sum_{\bar{I}=1}^{3} \lambda^{e2}_{\bar{I}} \bar{\boldsymbol{n}}_{\bar{I}} \otimes \bar{\boldsymbol{n}}_{\bar{I}}, \tag{3.20}$$

with $\lambda_{\bar{I}}$ being the positive eigenvalues and $\bar{\boldsymbol{n}}_{\bar{I}}$ being the orthonormal eigenvectors of $\boldsymbol{U}^e$. Note that $\boldsymbol{U}^e\bar{\boldsymbol{n}}_{\bar{I}} = \lambda^e_{\bar{I}}\bar{\boldsymbol{n}}_{\bar{I}}$ and $\bar{\boldsymbol{C}}^e\bar{\boldsymbol{n}}_{\bar{I}} = \lambda^{e2}_{\bar{I}}\bar{\boldsymbol{n}}_{\bar{I}}$. Here, we also introduce the principal elastic logarithmic strains $\bar{E}^e_{\bar{I}} = \ln \lambda^e_{\bar{I}}$, and consider the isotropy of $\hat{\bar{\Psi}}_e(\bar{\boldsymbol{C}}^e)$ to equivalently express it as: $\hat{\bar{\Psi}}_e(\bar{\boldsymbol{C}}^e) \rightarrow \breve{\bar{\Psi}}_e(\lambda^e_{\bar{I}}) \rightarrow \tilde{\bar{\Psi}}_e(\bar{E}^e_{\bar{I}})$. Therefore, the stress $\bar{\boldsymbol{S}}_A$, Eq.$(3.18)_1$, can be written as

$$\bar{\boldsymbol{S}}_A = 2\frac{\partial \hat{\bar{\Psi}}_e}{\partial \bar{\boldsymbol{C}}^e} = 2\sum_{\bar{I}=1}^{3} \frac{\partial \breve{\bar{\Psi}}_e(\lambda^e_{\bar{I}})}{\partial \lambda^e_{\bar{I}}} \frac{\partial \lambda^e_{\bar{I}}}{\partial \bar{\boldsymbol{C}}^e} = 2\sum_{\bar{I}=1}^{3} \frac{\partial \tilde{\bar{\Psi}}_e(\bar{E}^e_{\bar{I}})}{\partial \bar{E}^e_{\bar{I}}} \frac{\partial \bar{E}^e_{\bar{I}}}{\partial \lambda^e_{\bar{I}}} \frac{\partial \lambda^e_{\bar{I}}}{\partial \bar{\boldsymbol{C}}^e} \tag{3.21}$$

Noting that $\partial\lambda^e_{\bar{I}}/\partial\bar{\boldsymbol{C}}^e = \bar{\boldsymbol{n}}_{\bar{I}} \otimes \bar{\boldsymbol{n}}_{\bar{I}}/2\lambda^e_{\bar{I}}$ and $\partial\bar{E}^e_{\bar{I}}/\partial\lambda^e_{\bar{I}} = \lambda^{e-1}_{\bar{I}}$, we can simplify Eq.(3.21) to

$$\bar{\boldsymbol{S}}_A = \sum_{\bar{I}=1}^{3} \frac{1}{\lambda^{e2}_{\bar{I}}} \frac{\partial \tilde{\bar{\Psi}}_e(\bar{E}^e_{\bar{I}})}{\partial \bar{E}^e_{\bar{I}}} \bar{\boldsymbol{n}}_{\bar{I}} \otimes \bar{\boldsymbol{n}}_{\bar{I}} \tag{3.22}$$

Therefore the Mandel stress $\bar{\boldsymbol{M}}_A$ and kirchhoff stress $\boldsymbol{\tau}_A$ can be written as

$$\bar{\boldsymbol{M}}_A = \bar{\boldsymbol{C}}^e\bar{\boldsymbol{S}}_A = \sum_{\bar{I}=1}^{3} \frac{\partial \tilde{\bar{\Psi}}_e(\bar{E}^e_{\bar{I}})}{\partial \bar{E}^e_{\bar{I}}} \bar{\boldsymbol{n}}_{\bar{I}} \otimes \bar{\boldsymbol{n}}_{\bar{I}}, \qquad \boldsymbol{\tau}_A = \boldsymbol{F}^e\bar{\boldsymbol{S}}_A\boldsymbol{F}^{eT} = \boldsymbol{R}^e\bar{\boldsymbol{M}}_A\boldsymbol{R}^{eT} \tag{3.23}$$

Note that $\bar{\boldsymbol{M}}_A$ is symmetric. To obtain an explicit expression for $\bar{\boldsymbol{M}}_A$, one can consider the following simple generalization of the classical strain energy function of infinitesimal isotropic elasticity which uses a logarithmic measure of finite strain,

$$\tilde{\bar{\Psi}}_e(\bar{E}^e_{\bar{I}}) = \mu(\bar{E}^{e2}_1 + \bar{E}^{e2}_2 + \bar{E}^{e2}_3) + \frac{1}{2}(K - \frac{2}{3}\mu)(\bar{E}^e_1 + \bar{E}^e_2 + \bar{E}^e_3)^2 \tag{3.24}$$

where μ and K are the elastic shear and bulk moduli modeling the elastic behavior of branch A. Using this expression in Eq.$(3.23)_1$, one can write for the Mandel stress $\bar{\boldsymbol{M}}_A$,

$$\bar{\boldsymbol{M}}_A = 2\mu\bar{\boldsymbol{E}}^e + (K - \frac{2}{3}\mu)\overline{\mathrm{Tr}}(\bar{\boldsymbol{E}}^e)\mathbf{1}, \qquad \bar{\boldsymbol{E}}^e = \sum_{\bar{I}=1}^{3} \ln\lambda_{\bar{I}}^e\, \bar{\boldsymbol{n}}_{\bar{I}} \otimes \bar{\boldsymbol{n}}_{\bar{I}} = \ln \boldsymbol{U}^e \tag{3.25}$$

where $\mathbf{1} = \sum_{I=1}^{3} \bar{\boldsymbol{n}}_{\bar{I}} \otimes \bar{\boldsymbol{n}}_{\bar{I}}$ is the second order identity tensor, and $\overline{\mathrm{Tr}}(\bar{\boldsymbol{E}}^e) = \bar{\boldsymbol{E}}^e\mathbf{:}\mathbf{1}$. Equations (3.25) and $(3.23)_2$ completely define the nonlinear elastic response of branch A.

To determine the stress in branch B, we model the elastic response of the Langevin spring using finite strain elasticity with uncoupled, volumetric / deviatoric responses. For this purpose, we introduce the folowing volumetric / deviatoric multiplicative split of $\boldsymbol{F}$,

$$\boldsymbol{F} = J^{1/3}\boldsymbol{F}^*, \qquad \det\boldsymbol{F}^* = 1, \qquad J = \det\boldsymbol{F} \tag{3.26}$$

which results in the following expression for the right Cauchy-Green tensor $\boldsymbol{C}$

$$\boldsymbol{C} = \boldsymbol{F}^T\boldsymbol{F} = J^{2/3}\boldsymbol{C}^*, \qquad \boldsymbol{C}^* = \boldsymbol{F}^{*T}\boldsymbol{F}^*, \qquad J = (\det\boldsymbol{C})^{1/2} \tag{3.27}$$

To align with decomposition (3.26), one can use the following additive split for $\hat{\bar{\Psi}}_C(\boldsymbol{C})$

$$\hat{\bar{\Psi}}_C(\boldsymbol{C}) = \hat{\bar{\Psi}}_{C^*}(\boldsymbol{C}^*) + \hat{\bar{\Psi}}_J(J) \tag{3.28}$$

and introduce an effective distorsional stretch ratio defined by †

$$\bar{\lambda} = \frac{1}{\sqrt{3}}\sqrt{\mathrm{Tr}(\boldsymbol{C}^*)} \tag{3.29}$$

Then, using the isotropy of $\hat{\bar{\Psi}}_{C^*}(\boldsymbol{C}^*)$, one could express $\hat{\bar{\Psi}}_{C^*}(\boldsymbol{C}^*) \to \hat{\bar{\Psi}}_{\bar{\lambda}}(\bar{\lambda})$ and, hence, derive the following expression for the 2nd Piola-Kirchhoff $\boldsymbol{S}_B$

$$\boldsymbol{S}_B = 2\frac{\partial\hat{\bar{\Psi}}_C}{\partial\boldsymbol{C}}(\boldsymbol{C}) = 2\frac{\partial\hat{\bar{\Psi}}_{\bar{\lambda}}(\bar{\lambda})}{\partial\bar{\lambda}}\frac{\partial\bar{\lambda}}{\partial\boldsymbol{C}} + 2\frac{\partial\hat{\bar{\Psi}}_J(J)}{\partial J}\frac{\partial J}{\partial\boldsymbol{C}} \tag{3.30}$$

where, from Eq.(3.29),

$$\frac{\partial\bar{\lambda}}{\partial\boldsymbol{C}} = \frac{1}{6\bar{\lambda}}\mathrm{tr}\Big(\frac{\partial\boldsymbol{C}^*}{\partial\boldsymbol{C}}\Big) \tag{3.31}$$

†Consider the polar decomposition of $\boldsymbol{F}^* = \boldsymbol{R}^*\boldsymbol{U}^*$. The spectral decomposition of $\boldsymbol{U}^*$ and $\boldsymbol{C}^* = \boldsymbol{U}^{*2}$ can be written as

$$\boldsymbol{U}^* = \sum_{I=1}^{3} \lambda_I \boldsymbol{N}_I \otimes \boldsymbol{N}_I, \qquad \boldsymbol{C}^* = \sum_{I=1}^{3} \lambda_I^2 \boldsymbol{N}_I \otimes \boldsymbol{N}_I$$

where λ_I are the positive eigenvalues and $\boldsymbol{N}_I$ are the orthonormal eigenvectors of $\boldsymbol{U}^*$. Noting that $\mathrm{tr}(\boldsymbol{C}^*) = \sum_{I=1}^{3}\lambda_I^2\mathrm{Tr}(\boldsymbol{N}_I \otimes \boldsymbol{N}_I) = \sum_{I=1}^{3}\lambda_I^2$, one can defined an average or effective stretch $\bar{\lambda}$ as

$$\bar{\lambda}^2 = \frac{1}{3}\sum_{I=1}^{3}\lambda_I^2 \qquad \to \qquad \bar{\lambda} = \frac{1}{\sqrt{3}}\sqrt{\mathrm{Tr}(\boldsymbol{C}^*)}$$

Expressions for $\partial \boldsymbol{C}^*/\partial \boldsymbol{C}$ and $\partial J/\partial \boldsymbol{C}$ can be obtained from Eqs.(3.27) as [Simo and Hughes, 1998]

$$\frac{\partial \boldsymbol{C}^*}{\partial \boldsymbol{C}} = J^{2/3}(\boldsymbol{I} - \frac{1}{3}\boldsymbol{C} \otimes \boldsymbol{C}^{-1}), \qquad \frac{\partial J}{\partial \boldsymbol{C}} = \frac{1}{2} J \boldsymbol{C}^{-1} \tag{3.32}$$

By substituting these expressions into Eq.(3.30) and performing some algebraic manipulations, we can write for the stress $\boldsymbol{S}_B$,

$$\boldsymbol{S}_B = \mu_B \, \boldsymbol{C}^{-1} \mathrm{DEV} \boldsymbol{C}^* + \kappa_B \, \boldsymbol{C}^{-1} \tag{3.33}$$

where $\mathrm{DEV}(\bullet) = (\bullet) - 1/3\mathrm{Tr}(\bullet)\mathbf{1}$, $\mathrm{Tr}(\bullet) = (\bullet)\mathbf{:1}$. In this equation, the distorsional and volumetric elastic properties of the Langevin spring (rubbery behavior of the material) are represented by the shear modulus function μ_B and the bulk modulus function κ_B, respectively. These material functions are given by

$$\mu_B = \hat{\mu}_B(\bar{\lambda}) = \frac{1}{3\bar{\lambda}} \frac{\partial \hat{\bar{\Psi}}_{\bar{\lambda}}(\bar{\lambda})}{\partial \bar{\lambda}}, \qquad \kappa_B = \hat{\kappa}_B(J) = J \frac{\partial \hat{\bar{\Psi}}_J(J)}{\partial J} \tag{3.34}$$

By pushing forward Eq.(3.33) to the current configuration, we obtain the expression for the Kirchhoff stress $\boldsymbol{\tau}_B$ acting on the hyperelastic rubbery spring as

$$\boldsymbol{\tau}_B = \boldsymbol{F} \boldsymbol{S}_B \boldsymbol{F}^T = \hat{\mu}_B(\hat{\lambda}) \, \mathrm{dev} \boldsymbol{b}^* + \hat{\kappa}_B(J) \, \mathbf{1}, \tag{3.35}$$

where, as above, $\mathrm{dev}(\bullet) = (\bullet) - 1/3\mathrm{tr}(\bullet)\mathbf{1}$, $\mathrm{tr}(\bullet) = (\bullet)\mathbf{:1}$, and the effective stretch $\bar{\lambda}$ is now expressed as

$$\bar{\lambda} = \frac{1}{\sqrt{3}} \sqrt{\mathrm{tr}(\boldsymbol{b}^*)}, \qquad \boldsymbol{b}^* = \boldsymbol{F}^* \boldsymbol{F}^{*T} \tag{3.36}$$

As mentioned before, the hyperelastic stress response given by Eq.(3.33) or Eq.(3.35) models the strain hardening at finite strains due to chain-alignment of the polymer molecular network. This internal network stress, also called entropic (rubbery) restorative stress or back stress [Arruda and Boyce, 1993], will be fully specified once specific functional forms for $\hat{\bar{\Psi}}_{\bar{\lambda}}(\bar{\lambda})$ and $\hat{\bar{\Psi}}_J(J)$ are prescribed. In this respect, based on statistical mechanics models of rubber elasticity, a number of authors, e.g. [Anand and Ames, 2006], has considered for $\hat{\bar{\Psi}}_{\bar{\lambda}}(\bar{\lambda})$ the functional form

$$\hat{\bar{\Psi}}_{\bar{\lambda}}(\bar{\lambda}) = \mu_R \lambda_L^2 \Big[\frac{\bar{\lambda}}{\lambda_L} X + \ln\Big(\frac{X}{\sinh X}\Big) - \frac{1}{\lambda_L} Y - \ln\Big(\frac{Y}{\sinh Y}\Big) \Big] \tag{3.37}$$

$$X = \mathcal{L}^{-1}\Big(\frac{\bar{\lambda}}{\lambda_L}\Big), \qquad Y = \mathcal{L}^{-1}\Big(\frac{1}{\lambda_L}\Big) \tag{3.38}$$

where $\mathcal{L}^{-1}$ is the inverse of the Langevin function $\mathcal{L}(\bullet) = \coth(\bullet) - (\bullet)^{-1}$, and μ_R and λ_L are two material parameters called the rubbery modulus and the network locking stretch,

respectively. On the other hand, for $\hat{\bar{\Psi}}_J(J)$ we use the functional form [Simo and Hughes, 1998]

$$\hat{\bar{\Psi}}_J(J) = \frac{1}{2}K_B\Big[\frac{1}{2}(J^2-1) - \ln J\Big] \tag{3.39}$$

where K_B is an elastic bulk modulus. Hence, using Eqs.(3.34), (3.37) and (3.39), we obtain for the shear $\hat{\mu}_B(\bar{\lambda})$ and bulk $\hat{\kappa}_B(J)$ modulus functions

$$\mu_B = \hat{\mu}_B(\bar{\lambda}) = \mu_R\frac{\lambda_L}{3\bar{\lambda}}\mathcal{L}^{-1}\Big(\frac{\bar{\lambda}}{\lambda_L}\Big), \qquad \kappa_B = \hat{\kappa}_B(J) = \frac{1}{2}K_B(J^2-1), \tag{3.40}$$

expressions that together with Eq.(3.35) fully define the hyperelastic response of branch B.

To complement the constitutive description of amorphous polymers, we need to describe the response of the nonlinear viscous dashpot. This element should be able to capture the inelastic mechanisms present during the yield behavior of the polymeric material, mechanisms that are typically associated with the localized slip or viscous flow processes resulting from the permanent displacement of long-chain molecules with respect to each other. To capture these effects, the behavior of the dashpot is represented with the flow rule [Boyce, *et al.*, 1998; Anand and Ames, 2006]

$$\dot{\boldsymbol{F}}^p = \bar{\boldsymbol{D}}^p\boldsymbol{F}^p, \qquad \bar{\boldsymbol{D}}^p = \frac{1}{\sqrt{2}}\dot{\gamma}^p\bar{\boldsymbol{N}}^p, \tag{3.41}$$

where $\dot{\gamma}^p = \sqrt{2}\| \bar{\boldsymbol{D}}^p \|^{1/2}$, the equivalent plastic shear-strain rate, is given by the kinetic equation

$$\dot{\gamma}^p = \hat{\Phi}(\bar{\tau}_A, \bar{\pi}_A, \kappa), \tag{3.42}$$

and $\boldsymbol{N}^p$, a unit deviatoric tensor defining the direction of plastic flow, is defined by the symmetric deviatoric tensor $\overline{\mathrm{DEV}}\bar{\boldsymbol{M}}_A$, i.e.,

$$\bar{\boldsymbol{N}}^p = \frac{\overline{\mathrm{DEV}}\bar{\boldsymbol{M}}_A}{\| \overline{\mathrm{DEV}}\bar{\boldsymbol{M}}_A \|} \tag{3.43}$$

In Eq.(3.42), $\bar{\tau}_A$ and $\bar{\pi}_A$ are the effective shear stress and effective pressures, respectively, defined by

$$\bar{\tau}_A = \frac{1}{\sqrt{2}}\| \overline{\mathrm{DEV}}\bar{\boldsymbol{M}}_A \|, \qquad \bar{\pi}_A = -\frac{1}{3}\overline{\mathrm{Tr}}(\bar{\boldsymbol{M}}_A), \tag{3.44}$$

and κ is a stress-like internal state variable representing aspects of the molecular resistance to plastic flow associated with the inelastic mechanisms and whose evolution equation can in general be represented by

$$\dot{\kappa} = \hat{\Theta}(\kappa, \dot{\gamma}^p) \tag{3.45}$$

Note that Eq.(3.42) includes a pressure-dependence of the inelastic resistance to plastic flow, as espect that has been observed experimentally for isotropic amorphous polymeric materials subjected to moderately large hydrostatic pressures. Typical functional forms for $\hat{\Phi}$ and $\hat{\Theta}$ used in the literature are a power law form and a Voce's type hardening (softening) rule, respectively,

$$\hat{\Phi}(\bar{\tau}_A, \bar{\pi}_A, \kappa) = \dot{\gamma}_0 \Big(\frac{\bar{\tau}_A}{\kappa + \alpha \bar{\pi}_A} \Big)^{1/m}, \qquad \hat{\Phi}(\kappa, \dot{\gamma}^p) = h_0 \Big(1 - \frac{\kappa}{\kappa_S} \Big) \dot{\gamma}^p \tag{3.46}$$

where $\dot{\gamma}_0$ is a reference strain rate, m is a strain rate sensitivity parameter, α is a pressure sensitivity parameter, h_0 is a hardening (softening) modulus and κ_S is a saturation value of the molecular resistance to plastic flow. It is important to note here many polymeric materials show a strain–softening region in their stress–strain response just after yielding [Boyce, *et al.*, 1988]. Such an effect on the model response is incorporated using Eq.$(3.46)_2$ with an appropriate choice of h_0 while keeping $\kappa_0 > \kappa_S$. Here, κ_0 is the initial deformation resistance (shear yield strength) of the material.

A summary of the constitutive model for the viscoelastic-viscoplastic response of amorphous polymers is presented in Box 1.

Box 1. Constitutive Model for Glassy Polymers

Branch A:

$$\begin{aligned}
\boldsymbol{F}_A &= \boldsymbol{F} = \boldsymbol{F}^e\boldsymbol{F}^p, \qquad \boldsymbol{F}^e = \boldsymbol{R}^e\boldsymbol{U}^e \\
\boldsymbol{\tau}_A &= \boldsymbol{R}^e\bar{\boldsymbol{M}}_A\boldsymbol{R}^{eT}, \qquad \bar{\boldsymbol{M}}_A = 2\mu\ln\boldsymbol{U}^e + (K-\frac{2}{3}\mu)\,\overline{\mathrm{Tr}}(\ln\boldsymbol{U}^e)\mathbf{1} \\
\dot{\boldsymbol{F}}^p &= \bar{\boldsymbol{L}}^p\boldsymbol{F}^p \\
\bar{\boldsymbol{L}}^p &= \bar{\boldsymbol{D}}^p + \bar{\boldsymbol{W}}^p, \qquad \bar{\boldsymbol{D}}^p = \frac{1}{2}\dot{\gamma}^p\bar{\boldsymbol{N}}^p, \qquad \bar{\boldsymbol{W}}^p = 0 \\
\dot{\gamma}^p &= \hat{\Phi}(\bar{\tau}_A, \bar{\pi}_A, \kappa), \qquad \dot{\kappa} = \hat{\Theta}(\kappa, \dot{\gamma}^p)
\end{aligned}$$

where

$$\bar{\boldsymbol{N}}^p = \frac{\overline{\mathrm{DEV}}\bar{\boldsymbol{M}}_A}{\parallel \overline{\mathrm{DEV}}\bar{\boldsymbol{M}}_A \parallel}, \qquad \bar{\tau}_A = \frac{1}{\sqrt{2}}\parallel \overline{\mathrm{DEV}}\bar{\boldsymbol{M}}_A \parallel, \qquad \bar{\pi}_A = -\frac{1}{3}\overline{\mathrm{Tr}}(\bar{\boldsymbol{M}}_A)$$

Branch B:

$$\begin{aligned}
\boldsymbol{F}_B &= \boldsymbol{F} = J^{1/3}\boldsymbol{F}^*, \qquad \det\boldsymbol{F}^* = 1, \qquad \det\boldsymbol{F} = J \\
\boldsymbol{\tau}_B &= \mu_R\frac{\lambda_L}{3\bar{\lambda}}\mathcal{L}^{-1}\Big(\frac{\bar{\lambda}}{\lambda_L}\Big)\,\mathrm{dev}\boldsymbol{b}^* + \frac{1}{2}K_B(J^2-1)\mathbf{1}
\end{aligned}$$

where

$$\boldsymbol{b}^* = \boldsymbol{F}^*\boldsymbol{F}^{*T}, \qquad \bar{\lambda} = \frac{1}{\sqrt{3}}\sqrt{\mathrm{tr}\boldsymbol{b}^*}$$

Total Kirchhoff stress and Cauchy stress:

$$\boldsymbol{\tau} = \boldsymbol{\tau}_A + \boldsymbol{\tau}_B, \qquad \boldsymbol{\sigma} = J^{-1}\boldsymbol{\tau}$$

Material parameters: $\mu, K; \dot{\gamma}_0, \alpha, m; h_0, \kappa_S; \mu_R, \lambda_L, K_B.$

4. One–Dimensional Constitutive Model

4.1 Reduced Constitutive Equations

In this section we simplify the foregoing constitutive equations to the case of uniaxial loading. For this particular loading, the deformation is prescribed by

$$x_1 = \lambda_1 X_1, \qquad x_2 = \lambda_2 X_2, \qquad x_3 = \lambda_3 X_3, \qquad \lambda_2 = \lambda_3 \tag{4.1}$$

where X_I and x_i are the coordinates of the undeformed and deformed body configurations, respectively, and λ_I are the principal stretches. The deformation gradient $\boldsymbol{F}$ can then be computed as

$$\boldsymbol{F} = \frac{\partial \boldsymbol{x}}{\partial \boldsymbol{X}} = \begin{bmatrix} \lambda_1 & 0 & 0 \\ 0 & \lambda_2 & 0 \\ 0 & 0 & \lambda_2 \end{bmatrix}, \qquad J = \det \boldsymbol{F} = \lambda_1 \lambda_2^2 > 0, \qquad \lambda_1 > 0 \tag{4.2}$$

Note that for the deformation (4.2), we can write the polar decomposition of $\boldsymbol{F}$ as $\boldsymbol{F} = \boldsymbol{R}\boldsymbol{U} = \boldsymbol{U}$ since $\boldsymbol{R} = \boldsymbol{1}$. Also, here we simplify the problem by assuming a volume-preserving deformation, i.e., $J = 1$ (the reduced one-dimensional equations will not capture pressure effects on the response). This specific assumption implies that the stretches are related by $\lambda_2^2 = 1/\lambda_1$, and that, from Eq.(3.26), $\boldsymbol{F} = J^{1/3}\boldsymbol{F}^* = \boldsymbol{F}^*$. Introducing the notation $\lambda_1 = \lambda$, one can then express the velocity gradient $\boldsymbol{l} = \boldsymbol{d} + \boldsymbol{w}$, with $\boldsymbol{w} = \boldsymbol{0}$, and the tensor $\boldsymbol{b}^*$, Eq.$(3.36)_2$, as

$$\boldsymbol{l} = \boldsymbol{d} = \dot{\boldsymbol{F}}\boldsymbol{F}^{-1} = \frac{\dot{\lambda}}{\lambda}\mathbb{D}, \qquad \mathbb{D} = \begin{bmatrix} 1 & 0 & 0 \\ 0 & -\frac{1}{2} & 0 \\ 0 & 0 & -\frac{1}{2} \end{bmatrix} \tag{4.3}$$

and

$$\boldsymbol{b}^* = \boldsymbol{F}^*\boldsymbol{F}^{*T} = \begin{bmatrix} \lambda^2 & 0 & 0 \\ 0 & 1/\lambda & 0 \\ 0 & 0 & 1/\lambda \end{bmatrix} \tag{4.4}$$

This last expression implies that

$$\mathrm{tr}(\boldsymbol{b}^*) = \lambda^2 + \frac{2}{\lambda}, \qquad \mathrm{dev}\boldsymbol{b}^* = \frac{2}{3}\Big(\lambda^2 - \frac{1}{\lambda}\Big)\mathbb{D} \tag{4.5}$$

Therefore, the stress in branch B given by Eq.(3.35), with $\boldsymbol{\tau}_B = J\boldsymbol{\sigma}_B = \boldsymbol{\sigma}_B$, can be computed as

$$\boldsymbol{\sigma}_B = \frac{2}{3}\hat{\mu}_B(\bar{\lambda})\Big(\lambda^2 - \frac{1}{\lambda}\Big)\mathbb{D}, \qquad \bar{\lambda} = \frac{1}{\sqrt{3}}\Big(\lambda^2 + \frac{2}{\lambda}\Big) \tag{4.6}$$

with $\bar{\mu}_B(\bar{\lambda})$ obtained from Eq.$(3.40)_1$. To compute the stress in branch A, we express the elastic $\boldsymbol{F}^e$ and plastic $\boldsymbol{F}^p$ parts of $\boldsymbol{F}$, with $\boldsymbol{R}^e = \mathbf{1}$, as

$$\boldsymbol{F}^e = \boldsymbol{U}^e = \begin{bmatrix} \lambda_1^e & 0 & 0 \\ 0 & \lambda_2^e & 0 \\ 0 & 0 & \lambda_2^e \end{bmatrix} \qquad \boldsymbol{F}^p = \begin{bmatrix} \lambda_1^p & 0 & 0 \\ 0 & \lambda_2^p & 0 \\ 0 & 0 & \lambda_2^p \end{bmatrix} \tag{4.7}$$

Here, we let $\lambda_1^e = \lambda^e$, and since $J^e = J = 1$, we obtain $\lambda_2^{e2} = 1/\lambda^e$. Therefore the logarithmic strain, Eq.$(3.25)_2$, and the corresponding stress in branch A, Eq.$(3.23)_2$ with $\boldsymbol{\sigma}_A = J^e\boldsymbol{\tau}_A = \boldsymbol{\tau}_A = \bar{\boldsymbol{M}}_A$, are

$$\bar{\boldsymbol{E}}^e = \ln \boldsymbol{U}^e = \ln \lambda^e \mathbb{D} \qquad \rightarrow \qquad \boldsymbol{\sigma}_A = \bar{\boldsymbol{M}}_A = 2\mu \ln \lambda^e \mathbb{D} \tag{4.8}$$

To determine the expression for the flow rule, Eq.$(3.41)_1$, we denote $\lambda_1^p = \lambda^p$. Hence, since $J^p = 1$, we can also write $\lambda_2^{p2} = 1/\lambda^p$. Therefore, using Eq.$(4.7)_2$ we can write the flow rule as

$$\dot{\boldsymbol{F}}^p \boldsymbol{F}^{p-1} = \bar{\boldsymbol{D}}^p = \frac{\dot{\lambda}^p}{\lambda^p}\mathbb{D} \tag{4.9}$$

The expression for the plastic flow direction $\bar{\boldsymbol{N}}^p$ and the corresponding one for $\bar{\boldsymbol{D}}^p$ can be obtained from Eqs.(3.43) and $(3.41)_2$. For this purpose, we denote $\sigma_A = 2\mu \ln \lambda^e$. Then, using Eq.$(4.8)_2$ one obtains

$$\bar{\boldsymbol{N}}^p = \sqrt{\frac{2}{3}}\mathrm{sign}(\sigma_A) \qquad \rightarrow \qquad \bar{\boldsymbol{D}}^p = \frac{1}{\sqrt{3}}\dot{\gamma}^p \mathrm{sign}(\sigma_A)\mathbb{D} \tag{4.10}$$

where $\dot{\gamma}^p$ is given by Eq.(3.42) with

$$\bar{\tau}_A = \frac{\sqrt{3}}{2}|\sigma_A|, \qquad \bar{\pi}_A = 0 \tag{4.11}$$

A summary of the one-dimensional equations of the model is given in Box 2, where we have used Eqs.(3.46) and the notation $d_{11} = d = \dot{\epsilon}$ and $\bar{D}^p_{11} = \bar{D}^p$.

Box 2. One-Dimensional Constitutive Model

Applied Load:	$\dot{\lambda} = \dot{\epsilon}\lambda$
Branch A:	$\lambda = \lambda^e \lambda^p$
	$\sigma_A = 2\mu \ln(\lambda^e)$
	$\dot{\lambda}^p = \bar{D}^p \lambda^p$
	$\bar{D}^p = \frac{1}{\sqrt{3}} \dot{\gamma}^p \text{sign}(\sigma_A), \qquad \dot{\gamma}^p = \dot{\gamma}_0 \Big(\frac{\sqrt{3}}{2} \frac{\lvert\sigma_A\rvert}{\kappa} \Big)^{1/m}$
	$\dot{\kappa} = h_0 (1 - \frac{\kappa}{\kappa_S}) \dot{\gamma}^p$
Branch B:	$\sigma_B = \frac{2}{3} \hat{\mu}_B(\bar{\lambda}) \, (\lambda^2 - \lambda^{-1}), \qquad \bar{\lambda} = \frac{1}{\sqrt{3}} (\lambda^2 + 2\lambda^{-1})^{1/2}$
Cauchy Stress:	$\sigma = \sigma_A + \sigma_B$
Material Parameters:	$\mu, \dot{\gamma}_0, m, h_0, \kappa_S, \mu_R, \lambda_L.$

4.2 Numerical Integration of One–Dimensional Model

In this section we develop the numerical integration procedure for the one–dimensional constitutitve equations given in Box 2. This integration proceeds by discretizing the deformation history in time and numerically integrating the equations over each time step Δt. Denoting a general time step interval as $[t_n, t_{n+1}]$ with $t_{n+1} = t_n + \Delta t$, and using the subcripts n and $n+1$ to represent variables evaluated at t_n and t_{n+1}, we can write the integrated one–dimensional equations as

Applied load:

$$\lambda_{n+1} = \exp(\Delta t \, \dot{\epsilon}) \lambda_n, \qquad \text{or} \qquad \lambda_{n+1} = \exp(\dot{\epsilon} \, t_{n+1}) \tag{4.12}$$

Branch A:

$$\begin{aligned}
\lambda_{n+1} &= \lambda^e_{n+1} \lambda^p_{n+1} \\
\sigma_{A\,n+1} &= 2\mu \ln(\lambda^e_{n+1}) \\
\lambda^p_{n+1} &= \exp(\Delta t \bar{D}^p_{n+1}) \lambda^p_n \approx (1 + \Delta t \bar{D}^p_{n+1}) \lambda^p_n \\
\bar{D}^p_{n+1} &= \frac{1}{\sqrt{3}} \dot{\gamma}^p_{n+1} \text{sign}(\sigma_{A\,n}) \\
\dot{\gamma}^p_{n+1} &= \hat{\dot{\gamma}}^p(\sigma_{A\,n+1}, \kappa_{n+1}) = \dot{\gamma}_0 \Big(\frac{\sqrt{3}}{2} \frac{\lvert\sigma_{A\,n+1}\rvert}{\kappa_{n+1}} \Big)^{1/m}
\end{aligned} \tag{4.13}$$

$$\kappa_{n+1} \;=\; \kappa_n + h_0\Big(1 - \frac{\kappa_n}{\kappa_S}\Big)\Delta t\dot{\gamma}^p_{n+1}$$

Branch B:

$$\sigma_{B\,n+1} = \frac{2}{3}\bar{\mu}_B(\bar{\lambda}_{n+1})(\lambda^2_{n+1} - \lambda^{-1}_{n+1}), \qquad \bar{\lambda}_{n+1} = \frac{1}{\sqrt{3}}(\lambda^2_{n+1} + 2\lambda^{-1}_{n+1})^{1/2} \tag{4.14}$$

Cauchy Stress:

$$\sigma_{n+1} = \sigma_{A\,n+1} + \sigma_{B\,n+1} \tag{4.15}$$

where we have used a semi-implicit integration procedure [Moran, *et al.*, 1990] for the equations defining the behavior of branch A. This semi-implicit scheme is characterized for being implicit in the incremental plastic shear strain $\Delta\gamma^p$ and explicit in the flow direction and other variables. We note here that the above integration scheme assumes (*i*) that the deformation path represented by $\dot{\epsilon}$ is given, (*ii*) that the variables $(\sigma_{A\,n}, \lambda^p_n, \kappa_n)$ describing the response of branch A are known, and (*iii*) that the material parameters $(\mu, \dot{\gamma}_0,\, m,\, h,\, \kappa_S,\, \mu_R,\, \lambda_L)$ are input. Also note that while the response of branch B is fully determined once λ_{n+1} is known, computing the response of branch A requires an iterative procedure to compute the updated quantities $(\sigma_{A\,n+1}, \lambda^p_{n+1}, \kappa_{n+1})$. To develop this iterative scheme, we proceed by writing $\Delta\gamma^p_{n+1}$ as

$$\Delta\gamma^p_{n+1} = \Delta t\hat{\dot{\gamma}}^p(\sigma_{A\,n+1}, \kappa_{n+1}) \tag{4.16}$$

Using Eqns.(4.13), we can readily establish the functional dependence $\sigma_{A\,n+1} = \hat{\sigma}_A(\Delta\gamma^p_{n+1})$ and $\kappa_{n+1} = \hat{\kappa}(\Delta\gamma^p_{n+1})$. Then, from Eq.(4.16) we can write a residual as

$$\mathcal{R}_{\Delta\gamma^p,\,n+1} = \hat{\mathcal{R}}(\Delta\gamma^p_{n+1}) = \Delta\gamma^p_{n+1} - \Delta t\,\hat{\dot{\gamma}}^p(\hat{\sigma}_A(\Delta\gamma^p_{n+1}), \hat{\kappa}(\Delta\gamma^p_{n+1})) \tag{4.17}$$

which is used to devise a Newton-Raphson iterative scheme. The linearization of this residual gives

$$\Big[\underbrace{\frac{d\hat{\mathcal{R}}(\Delta\gamma^p_{n+1})}{d\Delta\gamma^p_{n+1}}}_{\partial_{\Delta\gamma^p}\mathcal{R}_{\Delta\gamma^p,\,n+1}}\Big] d\Delta\gamma^p_{n+1} = -\mathcal{R}_{\Delta\gamma^p,\,n+1} \tag{4.18}$$

where the Jacobian $\partial_{\Delta\gamma^p}\mathcal{R}_{\Delta\gamma^p,\,n+1}$ can be computed as

$$\frac{d\hat{\mathcal{R}}(\Delta\gamma^p_{n+1})}{d\Delta\gamma^p_{n+1}} = 1 - \Delta t\Big(\frac{\partial\dot{\gamma}^p_{n+1}}{\partial\sigma_{A\,n+1}}\frac{d\sigma_{A\,n+1}}{d\Delta\gamma^p_{n+1}} + \frac{\partial\dot{\gamma}^p_{n+1}}{\partial\kappa_{n+1}}\frac{d\kappa_{n+1}}{d\Delta\gamma^p_{n+1}}\Big) \tag{4.19}$$

The derivative $d\sigma_{A\,n+1}/d\Delta\gamma^p_{n+1}$ can be obtained from Eqs.$(4.13)_{1-4}$ as

$$\frac{d\sigma_{A\,n+1}}{d\Delta\gamma^p_{n+1}} = -\frac{2\mu}{\sqrt{3}}\Big[1 + \frac{\Delta t\dot{\gamma}^p_{n+1}}{\sqrt{3}}\text{sign}(\sigma_{A\,n})\Big]^{-1}\text{sign}(\sigma_{A\,n}) \tag{4.20}$$

To obtain the expressions for the partial derivatives $\partial\dot{\gamma}^p_{n+1}/\partial\sigma_{A\,n+1}$, $\partial\dot{\gamma}^p_{n+1}/\partial\kappa_{n+1}$ and the total derivative $d\kappa_{n+1}/d\Delta\gamma^p_{n+1}$ one needs to have the specific functional forms for the kinetic equation and hardening rule, respectively. For the particular case given by Eqs.$(4.13)_{4-5}$, these derivatives are determined as

$$\frac{\partial\dot{\gamma}^p_{n+1}}{\partial\sigma_{A\,n+1}} = \frac{\dot{\gamma}^p_{n+1}\text{sign}(\sigma_{A\,n+1})}{m|\sigma_{A\,n+1}|}, \qquad \frac{\partial\dot{\gamma}^p_{n+1}}{\partial\kappa_{n+1}} = -\frac{\dot{\gamma}^p_{n+1}}{m\kappa_{n+1}} \tag{4.21}$$

$$\frac{d\kappa_{n+1}}{d\Delta\gamma^p_{n+1}} = h_0(1-\frac{\kappa_n}{\kappa_S}) \tag{4.22}$$

Once $\Delta\gamma^p_{n+1}$ is computed by solving iteratively Eq.(4.18), from Eqs.(4.13) one can update the plastic λ^p_{n+1} and elastic λ^e_{n+1} stretches, and then the stress $\sigma_{A\,n+1}$ and hardness κ_{n+1}. Finally, one can compute the overall Cauchy stress σ_{n+1} using Eq.(4.15). A summary of this integration scheme is presented in Box 3, and the corresponding numerical implementation in MATLAB is documented in the appendix.

Box 3. Integration Procedure for One-Dimensional Model

1. Known quantities:
   $\dot{\epsilon};\ \sigma_{A\,n},\ \lambda^p_n,\ \kappa_n;$ material properties : $\mu;\dot{\gamma}_0,m;h,\kappa_S;\mu_R,\lambda_L.$

2. Compute total stretch λ_{n+1}:
   $\lambda_{n+1} = \exp(\dot{\epsilon}\,t_{n+1})$

3. Compute Cauchy stress in branch B:
   $\sigma_{B\,n+1} = 2/3\ \hat{\mu}_B(\bar{\lambda}_{n+1})(\lambda^2_{n+1}-\lambda^{-1}_{n+1})$
   where $\bar{\lambda}_{n+1}$ and $\hat{\mu}_B(\bar{\lambda}_{n+1})$ can be computed from Eqs.$(4.14)_2$ and $(3.40)_1$.

4. Compute Cauchy stress in branch A:

   (a) Compute $\Delta\gamma^p_{n+1}$ by solving iteratively (iteration (i)):
   $\Delta\gamma^{(i+1)}_{n+1} = \Delta\gamma^{(i)}_{n+1} - \left[\partial_{\Delta\gamma^p}\mathcal{R}^{(i)}_{\Delta\gamma^p,\,n+1}\right]^{-1}\mathcal{R}^{(i)}_{\Delta\gamma^p,\,n+1}$
   where $\mathcal{R}_{\Delta\gamma^p,\,n+1}$ and $\partial_{\Delta\gamma^p}\mathcal{R}_{\Delta\gamma^p,\,n+1}$ are given by Eqs.(4.17) and (4.19).

   (b) Update the plastic and elastic stretches:
   $\lambda^p_{n+1} = \left[1+\Delta\gamma^p_{n+1}\text{sign}(\sigma_{A\,n})/\sqrt{3}\right]\lambda^p_n, \qquad \lambda^e_{n+1} = \lambda_{n+1}\lambda^{p-1}_{n+1}$

   (c) Update stress and hardness:
   $\sigma_{A\,n+1} = 2\mu\ln(\lambda^e_{n+1}), \qquad \kappa_{n+1} = \kappa_n + h_0(1-\kappa_n/\kappa_S)\Delta\gamma^p_{n+1}$

5. Update total Cauchy stress:
   $\sigma_{n+1} = \sigma_{A\,n+1} + \sigma_{B\,n+1}$

4.3 Parametric Study based on One–Dimensional Model

In this section we carry out a parametric (sensitivity) study of the one–dimensional constitutive model to understand what salient features of the stress-strain response are affected when changing the values of the material parameters. This study assumes an isothermal uniaxial extension with an applied strain rate of $\dot{\epsilon} = 3 \times 10^{-4}\ \mathrm{s}^{-1}$. The nominal values of the material parameters chosen for this study are [Anand and Ames, 2006]

$$\begin{aligned} \mu &= 1.58 \times 10^3\,\mathrm{MPa} \\ \dot{\gamma}_0 &= 1 \times 10^{-4}\,\mathrm{s}^{-1} \\ m &= 0.265 \\ h_0 &= 250.0\ \mathrm{MPa} \\ \kappa_S &= 24.0\ \mathrm{MPa} \\ \kappa_0 &= 44.0\ \mathrm{MPa} \\ \lambda_L &= 1.65 \\ \mu_R &= 14.0\ \mathrm{MPa} \end{aligned}$$

Recall that the parameter μ defines the instantaneous elastic response of branch A, the constants for the flow rule ($\dot{\gamma}_0$, m) and hardening law (h_0, κ_S, κ_0) determine the viscous response of the dashpot, with κ_0 being the initial deformation resistance, and the parameters (λ_L, μ_R) describe the entropic hardening response (hyperelastic behavior) at large strains of branch B. Note that the combined response of the springs and dashpot will give the viscoelastic–viscoplastic behavior of the system. In what follows, we focus our attention on studying the effect of the parameters ($\dot{\gamma}_0, m$; h, κ_S, κ_0; μ_R, λ_L) on the strain-stress response. Note here that due to the assumptions imposed when deriving the reduced constitutive equations, i.e., $J = 1$, the one-dimensional model will not be able to capture pressure effects on the material response, and hence, the computed stress will mainly be deviatoric.

A typical true stress versus true strain curve in monotonic simple extension to a strain of 0.5 is shown in Fig. 4.1. This curve was computed with the nominal values of the parameters. After an approximately linear initial region, the stress-strain curve becomes nonlinear prior to reaching a peak in the stress at a strain of about 0.035. The material then strain-softens until a minimum in stress is reached at a strain of approximately 0.16. After this, the material exhibits a broad region of rapid strain hardening, as the stress once again rises because of the alignment and locking of the polymer chains. Hence, typical features observed experimentally in the mechanical behavior of many thermoplastic amorphous polymers are displayed by the computed response of the model: an initial elastic-viscoelastic response, followed by a nonlinear viscoelastic-viscoplastic behavior, a region of strain softening after yielding and finally subsequent strain hardening. Of course, the predominance of each of these features can be adjusted by varying the material parameters, as shown in the next figures.

The contribution of the stress in each branch to the total stress response is also displayed in Fig. 4.1. As shown, the stress in branch A dominates the overall response in the pre– and

post–yield regions until a minimum stress is reached during strain softening. The subsequent increase in stress level is due to the contribution of the hyperelastic stress response of branch B. This figure also shows the evolution of the strength resistance to plastic flow κ. As shown, the strength decays after a short transient from its initial value of $\kappa_0 = 44$ MPa to the saturation value of $\kappa_S = 24$ MPa. In fact, for the particular evolution law chosen for κ, Eq.$(3.46)_2$, the strain softening effect in the model is induced by keeping $\kappa_S < \kappa_0$.

The effect of the applied strain rate on the stress-strain curve is presented in Fig. 4.2, where the response of the model has been computed at two strain rates: $3 \times 10^{-4}\,\mathrm{s}^{-1}$ and $3 \times 10^{-5}\,\mathrm{s}^{-1}$. For the chosen nominal values of the parameters, we observe a strong rate dependence of the model response. In particular, increases in the applied strain rate result in increases of both the yield–peak and the level of post–yield strain softening. It is noted here that this rate dependent effect is tied to the parameters of the power–law flow rule, the rate sensitivity exponent m and the reference shear strain rate $\dot{\gamma}_0$. Figures 4.3–4.4 show the effect of changing the values of these parameters on the stress-strain response. As depicted in these figures, the rate dependence of the model response increases with increases in m and decreases in $\dot{\gamma}_0$, with the shape changes of the stress-curve curve being similar to the ones obtained when changing the applied strain rate.

The parameters defining the evolution law for the internal strength, the hardening–softening modulus h_0 and the deformation resistance saturation value κ_S, affect importantly the post–yield strain softening response, and to a lesser degree the yield peak or macroyielding. This can be observed from Figs. 4.5–4.6 that shows that the level of strain softening decreases as the value of h_0 decreases or the value of κ_S increases, while, at the same time, these changes affect slightly the transient peak associated with yielding. On the other hand, the initial deformation resistance κ_0 defines the shear yield strength of the material. As such, changing its values will mainly affect the yield peak or macro–yielding response, as shown in Fig. 4.7.

At large strains, the model response shows a rapid strain–hardening behavior. Physically, this hardening behavior is induced by the alignment of the macro–molecular network built of entangled polymer molecules, and it is typically associated with a decrease in the configurational entropy of the material. As mentioned before, such hardening effect is introduced in the model through a Langevin spring. Hence, the material parameters of this spring will define the level of strain hardening, as shown in Figs. 4.8–4.9, with the trend that this large-strain hardening effect gets more pronounced as the magnitude of λ_L is decreased or the value of μ_R is increased.

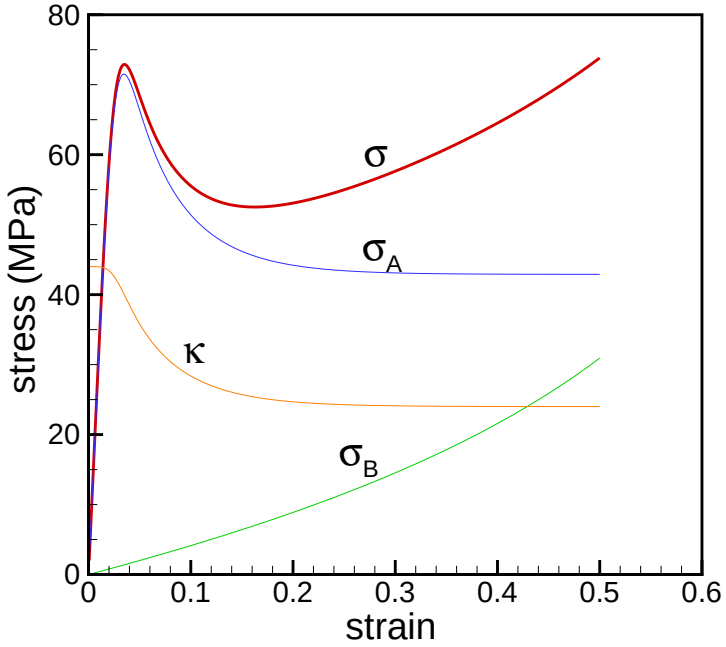

Figure 4.1: A typical stress–strain response numerically determined from the one–dimensional model: total stress σ and stresses in branches A, σ_A, and B, σ_B. The evolution of the strength κ is also shown.

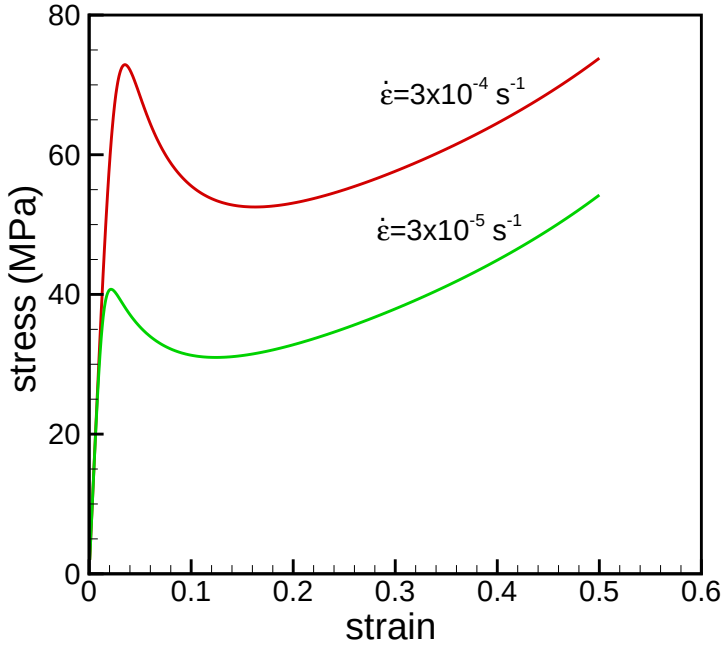

Figure 4.2: Effect of applied deformation rate $\dot{\epsilon}$ on the stress response.

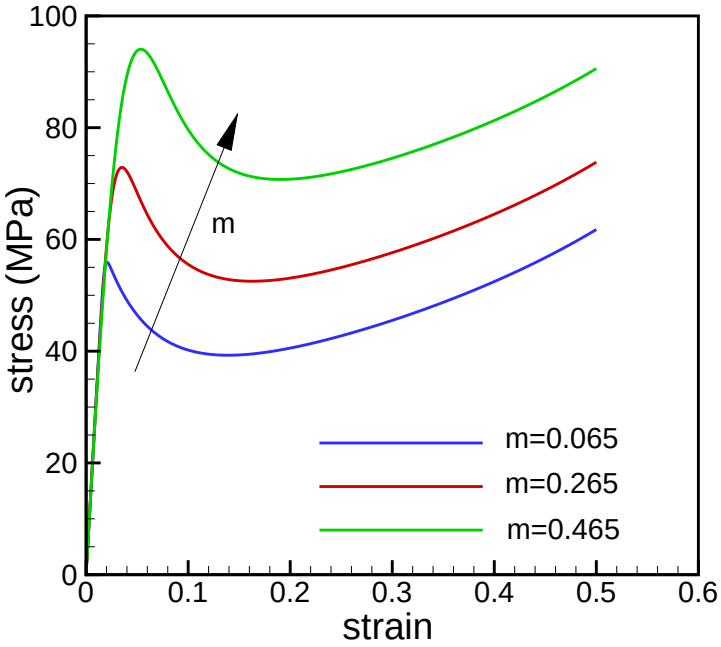

Figure 4.3: Effect of the rate sensitivity exponent m on the overall stress response.

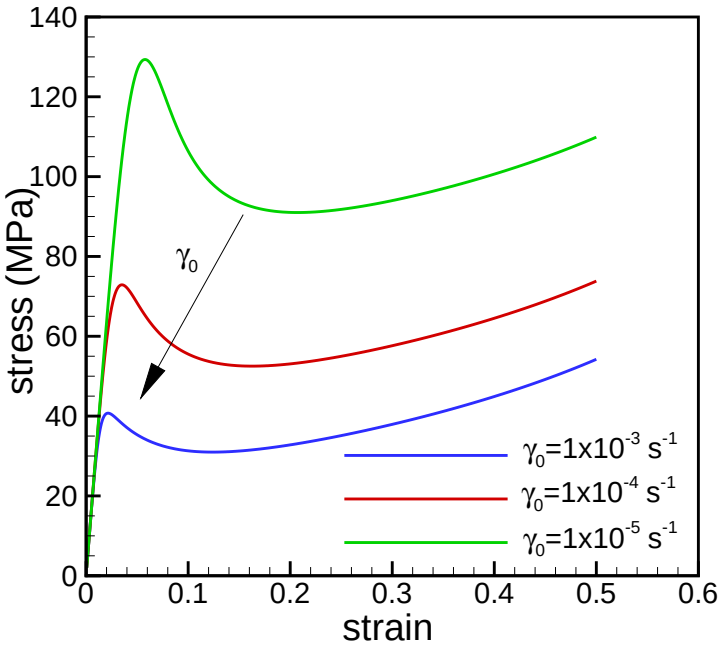

Figure 4.4: Effect of the reference shear strain rate $\dot{\gamma}_0$ on the overall stress response.

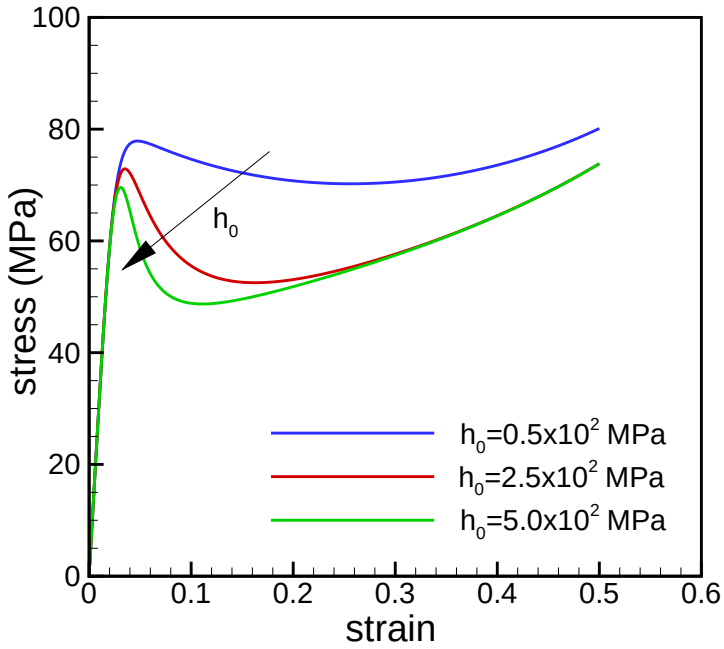

Figure 4.5: Effect of hardening (softening) modulus h_0 on the yield peak and post–yield behavior of the model.

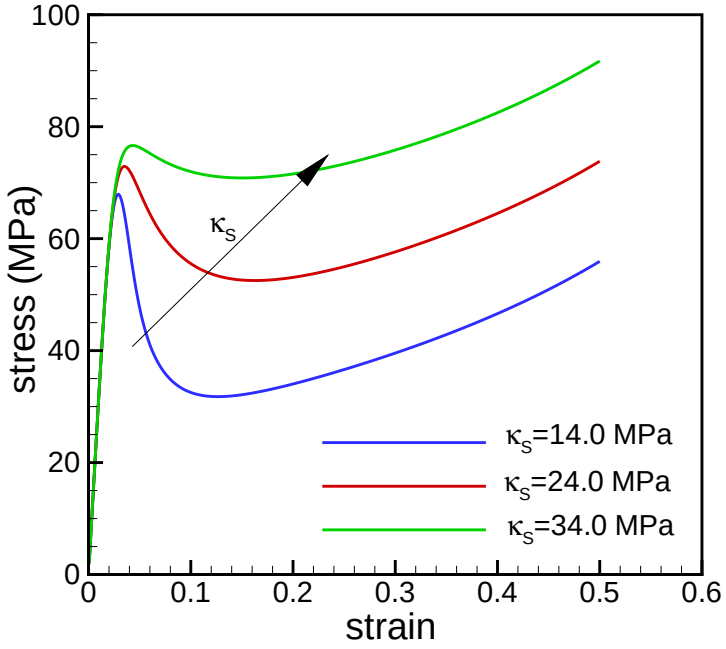

Figure 4.6: Effect of saturation value for the strength κ_S on the yield peak and post–yield response of the model.

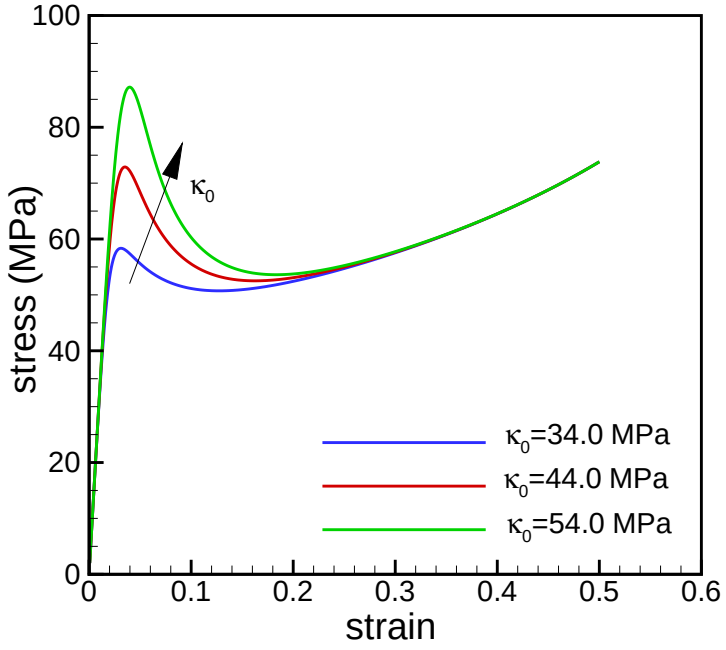

Figure 4.7: Effect of initial value of the strength κ_0 on the yield peak or macro–yielding response of the model.

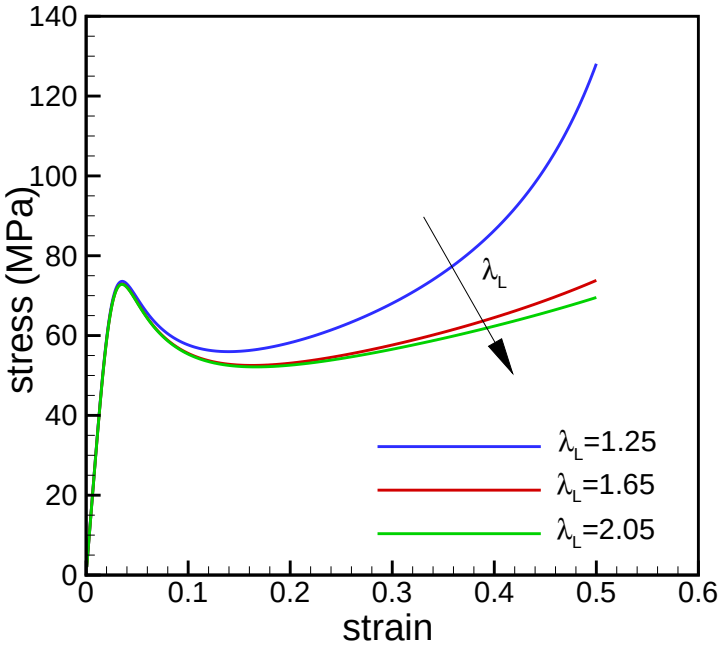

Figure 4.8: Effect of network locking stretch λ_L on the large strain hardening response of the model.

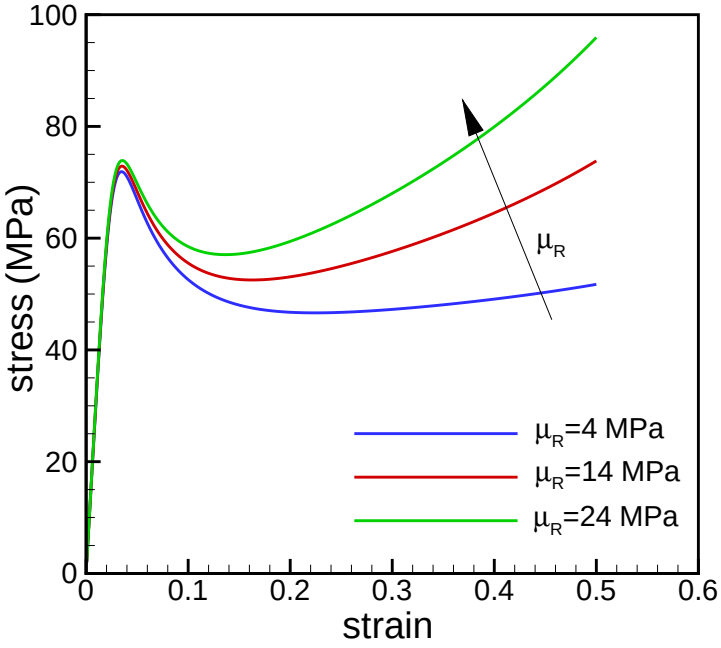

Figure 4.9: Effect of rubbery modulus μ_R on the large strain hardening response of the model.

5. Summary

A preliminary version of a three-dimensional viscoelastic-viscoplastic constitutive model for the isothermal, finite deformation of glassy polymers has been presented. The formulation has been developed in a thermodynamic framework and follows a widely used theory for amorphous polymers. Conceptually, the main components of the model consists of a nonlinear Maxwell element in parallel with a hyperelastic spring, an arrangement typically used to describe the constitutive behavior of amorphous polymers. A parametric study using the reduced one–dimensional constitutive equations has shown that major features of the stress-strain response of these thermoplastic polymeric materials are captured by the model: the plastic flow process, the post yield–strain softening behavior and the subsequent strain hardening at large strains. No attempt has been made to fit the model parameters to experimental data, as aspect that will be covered in a future report.

This work represents the initial steps at CAVS towards building a robust continuum internal state variable material model for predicting the response of polymeric–type materials for a broad range of temperatures and strain rates. The success of such modeling endeavours will depend, of course, to a large extent on the combination of theoretical and experimental efforts. From the theoretical viewpoint, a number of tasks can currently be identified. Among these are: (*i*) to develop a constitutive integration scheme for the three-dimensional equations and the corresponding numerical implementation in finite element codes, (*ii*) to devise a systematic parameter identification procedure in MATLAB using optimization techniques, and possibly, analytical sensitivity coefficients, and (*iii*) to identify the experimental tests needed for a complete evaluation of the model parameters. On the other hand, the experimental aspects of our modeling thrust should focus on building a material database that could be used to adapt the constitutive framework to fit the response of particular amorphous polymeric materials. Specific characterization experiments to be performed may initially include low–strain rate tests such as monotonic strain–controlled compression tests, cyclic strain–controlled compression–tension tests, and stress-controlled compression creep tests. In additon microindentation experiments may very well complement the experimental database and be used as a verification/validation experiment for the model predictions.

Finally, future work on polymers modeling should enhance and/or modify the presented constitutive framework to address (*a*) the effect of damage, temperature, pressure and anisotropy as well the behavior of mixed amorphous–crystalline polymers, and (*b*) the mechanical behavior of soft and hard biological tissues such as bones, ligaments, tendons and muscles. Such a continuum modeling framework will have important practical applications

to current research projects at CAVS which include modeling the behavior of polyurethane (a polymer used in run-flat insert tire designs) and predicting the response of human beings (biological tissues) in crash simulations.

6. References

Anand, L. (1996), "A Constitutive Model for Compressible Elastomeric Solids," *Computational Mechanics*, Vol. 18, pp. 339–355.

Anand, L. and Gurtin, M. E. (2005), "A Theory of Amorphous Solids Undergoing Large Deformations, with Application to Polymeric Glasses," *International Journal of Solids and Structures*, Vol. 40, pp. 1465–1487.

Anand, L. and Ames, N. M. (2006), "On Modeling the Micro-Indentation Response of an Amorphous Polymer," *International Journal of Plasticity*, Vol. 22, pp. 1123–1170.

Arruda, E. M., and Boyce, M. C., (1993), "A Three-Dimensional Constitutive Model for the Large Stretch Behavior of Rubber Elastic Materials", *Journal of the Mechanics and Physics of Solids*, 41:389–412.

Bardenhagen, S. G., Stout, M. G., and Gray, G. T., (1997), "Three–Dimensional, Finite Deformation, Viscoplastic Constitutive Models for Polymeric Materials", *Mechanics of Materials*, 25:235–253.

Boyce, M. C., Parks, D. M., and Argon, A. S., (1988), "Large Inelastic Deformation of Glassy Polymers. Part I: Rate Dependent Constitutive Model," *Mechanics of Materials*, 7:15–33.

Coleman, B., and Gurtin, M., (1967), "Thermodynamics With Internal State Variables", *J. Chem. Phys.*, 47:597–613.

Gurtin, M., (1981), "An Introduction to Continuum Mechanics" Academic Press.

Gurtin, M. E. and Anand, L. (2005), "The Decomposition $\boldsymbol{F} = \boldsymbol{F}^e\boldsymbol{F}^p$, Material Symmetry, and Plastic Irrotationality for Solids that are Isotropic-Viscoplastic or Amorphous," *International Journal of Plasticity*, Vol. 21, pp. 1686–1719.

Holzapfel, G. A., (2000), "Nonlinear Solid Mechanics. A Continuum Approach for Engineering", J. Wiley & Sons, Ltd.

Kontou, E., (2006), "Viscoplastic Deformation of an Epoxy Resin at Elevated Temperatures", *Journal of Applied Polymer Science*, 101:2027–2033.

Moran, B., Ortiz, M., and Shih, C. F., (1990), "Formulation of Implicit Finite Element Methods for Multiplicative Finite Deformation Plasticity," *Int. J. for Numerical Methods in*

Engng., 29:483–514.

Simo, J. C., and Hughes, T. J. R., (1998), "Computational Inelasticity", Springer.

Reese, S., and Govindjee, S., (1998), "A Theory of Finite Viscoelasticity and Numerical Aspects", *Int. J. of Solids and Structures*, 35:3455–3482.

Zairi, F., Nait-Abdelaziz, M., Woznica, K., and Gloaguen, J.-M., (2006), "Elasto-Viscoplastic Constitutive Equations for the Description of Glassy Polymers Behavior at Constant Strain Rate", *Journal of Engineering Materials and Technology*, 129:29–35.

7. Appendix

This appendix presents the MATLAB implementation of the numerical integration scheme described by Box 3. This implementation has been used to perform the parametric study of the one-dimensional constitutive model.

```
%%%%%%%%%%%%%%%%%%%%%%%%%%%%%%%%%%%%%%%%%%%%%%%%%%%%%%%%%%%%%%%%%%%%%%%%
% Implementation of preliminary version of one-dimensional (1-D)
% viscoelastic-viscoplastic model. The model follows closely
% Anand's formulation. The integration of the 1-D equations -
% branch A - is performed using a semi-implicit scheme. The
% reduced equations do not capture pressure effects.
%%%%%%%%%%%%%%%%%%%%%%%%%%%%%%%%%%%%%%%%%%%%%%%%%%%%%%%%%%%%%%%%%%%%%%%%

% Material properties

mu      = 1.58d3;   % shear modulus (MPa)
gamma0  = 1d-4;     % reference shear strain rate (1/s)
m       = 0.265;    % strain-rate sensitivity exponent
h_0     = 2.5d2;    % hardening modulus (MPa)
kappa_sat = 24.d0;  % saturation level of strength (MPa)
kappa_0   = 44;     % initial strength (MPa)

lambda_L = 1.65d0;  % rubbery modulus (MPa)
mu_R     = 14.0d0;  % network locking stretch

% Some numerical constants

SMALL = 1.d-16;     % a small number
RTOLER = 1.d-8;     % rel. tolerance for Newton's iters
ATOLER = 1.d-8;     % abs. tolerance for Newton's iters

% Deformation Path

e_dot  = 3.d-4;     % strain rate
```

```
e_max  = 0.5;       % max strain
Nincrs = 800;       % number of increments

N  = Nincrs;
t  = zeros(N,1);
e  = zeros(N,1);
dt = zeros(N,1);

t_max  = abs(e_max/e_dot);
delt_t = t_max / N;
delt_e = e_dot * delt_t;

for i = 1:N
  e(i)  = i*delt_e;
  dt(i) = delt_t;
end

% Initializations

tauA_n     = SMALL;
kappa_n    = kappa_0;
lambda_p_n = 1.0;
dgam_n     = SMALL;

fullData1 = [];

% Integrate model for given deformation history

time = 0.d0;
numIters = 100;

for i = 1:N

%   Time step and total time

    dtime = dt(i);
    time  = time + dt(i);
    t(i)  = time;

%   Total stretch at time t

    lambda = exp(e(i));
```

```
%   Calculate stress due to B system

    lambda_bar = sqrt(lambda*lambda + 2/lambda)/sqrt(3);
    arg = lambda_bar / lambda_L;
    if ( 0 < abs(arg) < 0.84136d0 )
       invLang = 1.31446d0 * tan(1.58986d0*arg) + 0.91209d0 * arg;
    elseif (abs(arg) < 1.0 )
       invLang =  1.d0/(sign(arg) - arg);
    else
       'error in inverse langevin argument'
    end
    mu_B  = mu_R * lambda_L / (3.d0*lambda_bar) * invLang;
    tauB = 2./3. * mu_B * (lambda*lambda - 1/lambda);

%   Calculate stress due to A system

%---- Initial guess for dgam

    dgam = dgam_n;

%---- Compute initial residual

    lambda_p = (1 + dgam*sign(tauA_n)/sqrt(3)) * lambda_p_n;
    lambda_e = lambda / lambda_p;
    tauA     = 2*mu*log(lambda_e);
    kappa    = kappa_n + h_0*(1-kappa_n/kappa_sat)*dgam;
    gammaDot = gamma0 * ( sqrt(3)/2 * abs(tauA)/kappa )^(1/m);
    resid    = dgam - dtime * gammaDot;
    resid0   = resid;
    res_0    = resid;

%---- Newton's iteration to compute incremental plastic shear strain

    converged = 0;
    iters     = 0;

    while ( (converged == 0) & (iters < numIters) )

        iters = iters + 1;
        dgam0 = dgam;
```

```
%-------- Compute Jacobian

        DgamdotDtauA = gammaDot * sign(tauA) / (m * abs(tauA));
        DgamdotDkapp = - gammaDot / (m * kappa);

        DtauADdgam = -2/sqrt(3) * mu * sign(tauA_n) / ...
                          ( 1 + dtime*gammaDot*sign(tauA_n)/sqrt(3) );
        DkappDdgam = h_0 * (1 - kappa_n/kappa_sat);

        jac = 1 - dtime * ( DgamdotDtauA * DtauADdgam ...
                                        + DgamdotDkapp * DkappDdgam );
        if (abs(jac) < SMALL)
          'Warning: Jacobian < SMALL'
        end

%-------- Compute incremental dgam and update

        ddgam = - resid / jac;
        search = 1;
        dgam = dgam0 + search*ddgam;
        if (dgam < 0.0)
           dgam = SMALL;
        end

%-------- New residual

        lambda_p = (1 + dgam*sign(tauA_n)/sqrt(3))*lambda_p_n;
        lambda_e = lambda / lambda_p;
        tauA     = 2*mu*log(lambda_e);
        kappa    = kappa_n + h_0*(1-kappa_n/kappa_sat)*dgam;
        gammaDot = gamma0 * ( sqrt(3)/2 * abs(tauA)/kappa )^(1/m);
        resid    = dgam - dtime * gammaDot;

%-------- Simple line search

        while ( abs(resid) > abs(resid0) )
            search = search*0.5;
            if (search < SMALL)
              'Warning: search < SMALL'
            end
            dgam = dgam0 + search*ddgam;
            if (dgam < 0.0) dgam = SMALL; end
```

```
            lambda_p = (1 + dgam*sign(tauA_n)/sqrt(3))*lambda_p_n;
            lambda_e = lambda / lambda_p;
            tauA     = 2*mu*log(lambda_e);
            kappa    = kappa_n + h_0*(1-kappa_n/kappa_sat)*dgam;
            gammaDot = gamma0 * ( sqrt(3)/2 * abs(tauA)/kappa )^(1/m);
            resid    = dgam - dtime * gammaDot;
        end

        resid0 = resid;

        if (abs(resid) < abs(res_0)*RTOLER | abs(resid) < ATOLER)
           converged = 1;
        end
    end

    if (iters >= numIters)
       'Warning: iters >= numIters'
    end

%---- Update variables

    lambda_p = (1 + dgam*sign(tauA_n)/sqrt(3))*lambda_p_n;
    lambda_e = lambda / lambda_p;
    tauA     = 2*mu*log(lambda_e);
    kappa    = kappa_n + h_0*(1-kappa_n/kappa_sat)*dgam;
    gammaDot = dgam / dtime;

    tauA_n     = tauA;
    kappa_n    = kappa;
    lambda_p_n = lambda_p;
    dgam_n     = dgam;

    tau = tauA + tauB;

%---- Save variables

    fullData1(i,1) = e(i);
    fullData1(i,2) = tau;
    fullData1(i,3) = tauA;
    fullData1(i,4) = tauB;
    fullData1(i,5) = kappa;
```

```
end

save -ascii visco_stress_semi fullData1;

figure(10)
   clf
   set(10, 'Position', [60 470 560 420])
   xlabel('strain')
   ylabel('stress')
   hold on

   plot((fullData1(:,1)), fullData1(:,2),'r-')
   plot((fullData1(:,1)), fullData1(:,3),'b-')
   plot((fullData1(:,1)), fullData1(:,4),'m-')
   plot((fullData1(:,1)), fullData1(:,5),'rx')

   legend( 'tau',  'tauA', 'tauB', 'kappa')
   title('stress response - semi-implicit integration.')
hold off
```